
Accelerated Information Gradient flow

Yifei Wang

School of Mathematical Sciences
Peking University
zackwang24@pku.edu.cn

Wuchen Li

Department of Mathematics
UCLA
wcli@math.ucla.edu

Abstract

We present a framework for Nesterov’s accelerated gradient flows in probability space. Here four examples of information metrics are considered, including Fisher-Rao metric, Wasserstein-2 metric, Kalman-Wasserstein metric and Stein metric. For both Fisher-Rao and Wasserstein-2 metrics, we prove convergence properties of accelerated gradient flows. In implementations, we propose a sampling-efficient discrete-time algorithm for Wasserstein-2, Kalman-Wasserstein and Stein accelerated gradient flows with a restart technique. We also formulate a kernel bandwidth selection method, which learns the gradient of logarithm of density from Brownian-motion samples. Numerical experiments, including Bayesian logistic regression and Bayesian neural network, show the strength of the proposed methods compared with state-of-the-art algorithms.

1 Introduction

Optimization problems in probability space, arising from Bayesian inference [16] and inverse problems [30], attract increasing attentions in machine learning communities [14, 4, 37]. One typical example here is to draw samples from an intractable target distribution. Such sampling problem is important in providing exploration in distribution of interest and quantifying uncertainty among data. From an optimization viewpoint, this problem suffices to minimize an objective functional, such as Kullback-Leibler (KL) divergence, which is to measure the closeness between current density and the target distribution.

Gradient descent methods play essential roles in solving these optimization problems. Here the gradient direction relies on the information metric in probability space. In literature, two important metrics, such as Fisher-Rao metric and Wasserstein-2 (in short, Wasserstein) metric, are of great interests [12, 1, 23]. The information gradient direction in terms of density corresponds to the update rule in a set of samples. This is known as sampling formulation or particle implementation of gradient flow, which yields various sampling algorithms. For Fisher-Rao metric, its gradient flow relates to birth-death dynamics, which is important in model selection and modeling population games [2]. The Fisher-Rao gradient, also known as natural gradient, is also useful in designing fast and reliable algorithms in probability models [1, 11, 20, 21]. For Wasserstein metric, the gradient flow of KL divergence is the Fokker-Planck equation of overdamped Langevin dynamic. In sampling algorithms, the time discretization of overdamped Langevin dynamics yields the classical Langevin Markov chain Monte Carlo (MCMC) method and the proximal Langevin algorithm [4, 37]. In recent years, various first-order sampling methods via generalized Wasserstein gradient direction are proposed. For example, the Stein variational gradient descent [16] formulates kernelized interacting Langevin dynamics. The Kalman-Wasserstein gradient, also known as ensemble Kalman sampling [10], induces covariance-preconditioned mean-field interacting Langevin dynamics.

For classical optimization problems in Euclidean space, the Nesterov’s accelerated gradient method [22] is a wide-applied optimization method and it accelerates gradient descent methods. The continuous-time limit of this method is known as the accelerated gradient flow [31]. Natural ques-

tions arise: *What is the accelerated gradient flow in probability space under general information metrics? What is the corresponding discrete-time sampling algorithm?* For optimization problems on a Riemannian manifold, accelerated gradient methods are studied in [17, 38]. The probability space embedded with information metric can be viewed as a Riemannian manifold, known as density manifold [12]. Several previous works explore accelerated methods in this manifold under Wasserstein metric. An acceleration framework of particle-based variational inference (ParVI) methods is proposed in [14, 13] based on manifold optimization. Taghvaei and Mehta [32] introduce accelerated flows from an optimal control perspective. Similar dynamics has been studied from a fluid dynamics viewpoint [5]. Underdamped Langevin dynamics is another way to accelerate on MCMC [6, 18].

In this paper, we present a unified framework of accelerated gradient flows in probability space embedded with information metrics, named Accelerated Information Gradient (AIG) flows. From a transport-information-geometry perspective, we derive AIG flows by damping Hamiltonian flows. Examples include Fisher-Rao metric, Wasserstein-2 metric, Kalman-Wasserstein metric and Stein metric. We rigorously prove the convergence rate of AIG flows based on the geodesic convexity of the loss function under both Fisher-Rao metric and Wasserstein metric. Besides, we handle two difficulties in numerical implementations of AIG flows under Wasserstein metric for sampling. On the one hand, as pointed out in [13, 32], the logarithm of density term (gradient of KL divergence) is difficult to approximate in particle formulations. We propose a novel kernel selection method, whose bandwidth is learned by sampling from Brownian motions. We call it the BM method. On the other hand, we notice that the AIG flow can be a numerically stiff system, especially in high-dimensional sample spaces. This is because the solution of AIG flows can be close to the boundary of the probability space. To handle this issue, we propose an adaptive restart technique, which accelerates and stabilizes the discrete-time algorithm. Numerical results in Bayesian Logistic regression and Bayesian neural networks indicate the validity of the BM method and the acceleration effects of proposed AIG flows.

This paper is organized as follows. Section 2 briefly reviews gradient flows and accelerated gradient flows in Euclidean space. Then, the information metrics in probability space and their corresponding gradient and Hamiltonian flows are introduced. In Section 3, we formulate AIG flows, under Fisher-Rao metric, Wasserstein metric, Kalman-Wasserstein metric and Stein metric. We theoretically prove the convergence rate of AIG flows in Section 4. Section 5 presents the discrete-time algorithm for W-AIG flows, including the BM method and the adaptive restart technique. Section 6 provides numerical experiments. In supplementary materials, we also provide discrete-time algorithms for both Kalman-Wasserstein AIG and Stein AIG flows.

2 Reviews

In this section, we review gradient flows and accelerated gradient flows in Euclidean space. Then, we introduce the optimization problems in probability spaces, and review several definitions of information metrics therein. Based on these metrics, we demonstrate gradient and Hamiltonian flows in probability space. These formulations serve necessary preparations for us to derive accelerated gradient flows in probability space. See detailed analysis on metrics in probability space in [3, 27, 29].

2.1 Accelerated gradient flows in Euclidean space

Consider an optimization problem in Euclidean space:

$$\min_{x \in \mathbb{R}^n} f(x),$$

where $f(x)$ is a given convex function with L -Lipschitz continuous gradient. $\langle \cdot, \cdot \rangle$ and $\| \cdot \|$ are the Euclidean inner product and norm in \mathbb{R}^n . The gradient descent method has the update rule

$$x_{k+1} = x_k - \tau_k \nabla f(x_k),$$

where $\tau_k > 0$ is a step size. With the limit $\tau_k \rightarrow 0$, the continuous-time limit of gradient descent method is the gradient flow (GF)

$$\dot{x}_t = -\nabla f(x_t).$$

To accelerate the gradient descent method, Nesterov introduced an accelerated method [22]:

$$\begin{cases} \mathbf{x}_k = \mathbf{y}_{k-1} - \tau_k \nabla f(\mathbf{y}_{k-1}), \\ \mathbf{y}_k = \mathbf{x}_k + \alpha_k (\mathbf{x}_k - \mathbf{x}_{k-1}). \end{cases}$$

Here α_k depends on the convexity of $f(x)$. If $f(x)$ is β -strongly convex, then $\alpha_k = \frac{\sqrt{L}-\sqrt{\beta}}{\sqrt{L}+\sqrt{\beta}}$; otherwise, $\alpha_k = \frac{k-1}{k+2}$. [31] show that the continuous-time limit of Nesterov's accelerated method satisfies an ODE, which is known as the accelerated gradient flow (AGF):

$$\ddot{x}_t + \alpha_t \dot{x}_t + \nabla f(x_t) = 0. \quad (1)$$

Here $\alpha_t = 2\sqrt{\beta}$ if $f(x)$ is β -strongly convex; $\alpha_t = 3/t$ for general convex $f(x)$.

An important observation in [19] is that the accelerated gradient flow (1) can be formulated as a damped Hamiltonian flow:

$$\begin{bmatrix} \dot{x}_t \\ \dot{p}_t \end{bmatrix} + \begin{bmatrix} 0 \\ \alpha_t p_t \end{bmatrix} - \begin{bmatrix} 0 & I \\ -I & 0 \end{bmatrix} \begin{bmatrix} \nabla_x H^E(x_t, p_t) \\ \nabla_p H^E(x_t, p_t) \end{bmatrix} = 0.$$

where x is the state variable and p is the momentum variable. The Hamiltonian function satisfies $H^E(x, p) = \frac{\|p\|^2}{2} + f(x)$, which consists of Euclidean kinetic function $\frac{\|p\|^2}{2}$ and potential function $f(x)$. In other words, one can formulate an accelerated gradient flow by adding a linear momentum term into the Hamiltonian flow. Later on, we follow this damped Hamiltonian perspective and derive related accelerated gradient flows in probability space.

2.2 Metrics in probability space

In practice, machine learning problems, especially Bayesian sampling problems, can be formulated as optimization problems in probability space. In other words, consider

$$\min_{\rho \in \mathcal{P}(\Omega)} E(\rho),$$

where $\Omega \subset \mathbb{R}^n$ is a region and the set of probability density is denoted by $\mathcal{P}(\Omega) = \{\rho \in \mathcal{F}(\Omega) : \int_{\Omega} \rho dx = 1, \rho \geq 0\}$. Here $\mathcal{F}(\Omega)$ represents the set of smooth functions on Ω . In practice, $E(\rho)$ is often chosen as a divergence or metric functional between ρ and a target density $\rho^* \in \mathcal{P}(\Omega)$.

In literature, it has been shown that various sampling algorithms correspond to gradient flows of $E(\rho)$, depending on the metrics in probability space. We brief review the definition of metrics in probability space as follows.

Definition 1 (Metric in probability space) Denote the tangent space at $\rho \in \mathcal{P}(\Omega)$ by $T_{\rho}\mathcal{P}(\Omega) = \{\sigma \in \mathcal{F}(\Omega) : \int \sigma dx = 0\}$. The cotangent space at ρ , $T_{\rho}^*\mathcal{P}(\Omega)$, can be treated as the quotient space $\mathcal{F}(\Omega)/\mathbb{R}$. A metric tensor $G(\rho) : T_{\rho}\mathcal{P}(\Omega) \rightarrow T_{\rho}^*\mathcal{P}(\Omega)$ is an invertible mapping from $T_{\rho}\mathcal{P}(\Omega)$ to $T_{\rho}^*\mathcal{P}(\Omega)$. This metric tensor defines the metric (inner product) on tangent space $T_{\rho}\mathcal{P}(\Omega)$:

$$g_{\rho}(\sigma_1, \sigma_2) = \int \sigma_1 G(\rho) \sigma_2 dx = \int \Phi_1 G(\rho)^{-1} \Phi_2 dx, \quad \sigma_1, \sigma_2 \in T_{\rho}\mathcal{P}(\Omega)$$

where Φ_i is the solution to $\sigma_i = G(\rho)^{-1} \Phi_i$, $i = 1, 2$.

Along with a given metric, the probability space $\mathcal{P}(\Omega)$ can be viewed as an infinite-dimensional Riemannian manifold, which is known as the density manifold [12]. We review four examples of metrics in $\mathcal{P}(\Omega)$: the Fisher-Rao metric from information geometry, the Wasserstein metric from optimal transport, the Kalman-Wasserstein metric from ensemble Kalman sampling and the Stein metric from Stein variational gradient method. For simplicity, we denote $\mathbb{E}_{\rho}[\Phi] = \int \Phi \rho dx$.

Example 1 (Fisher-Rao metric) The inverse of Fisher-Rao metric tensor is defined by

$$G^F(\rho)^{-1} \Phi = \rho (\Phi - \mathbb{E}_{\rho}[\Phi]), \quad \Phi \in T_{\rho}^*\mathcal{P}(\Omega).$$

Example 2 (Wasserstein metric) The inverse of Wasserstein metric tensor writes

$$G^W(\rho)^{-1} \Phi = -\nabla \cdot (\rho \nabla \Phi), \quad \Phi \in T_{\rho}^*\mathcal{P}(\Omega).$$

Example 3 (Kalman-Wasserstein metric, [10]) The inverse of metric tensor is defined by

$$G^{KW}(\rho)^{-1} \Phi = -\nabla \cdot (\rho C^{\lambda}(\rho) \nabla \Phi), \quad \Phi \in T_{\rho}^*\mathcal{P}(\Omega).$$

Here $\lambda \geq 0$ is a given regularization constant and $C^{\lambda}(\rho) \in \mathbb{R}^{n \times n}$ follows

$$C^{\lambda}(\rho) = \int (x - m(\rho))(x - m(\rho))^T \rho dx + \lambda I, \quad m(\rho) = \int x \rho dx.$$

Example 4 (Stein metric, [15, 9]) The inverse of Stein metric tensor is defined by

$$G^S(\rho)^{-1}\Phi(x) = -\nabla_x \cdot \left(\rho(x) \int k(x, y) \rho(y) \nabla_y \Phi(y) dy \right).$$

Here $k(x, y)$ is a given positive kernel function.

2.3 Gradient flows and Hamiltonian flows in probability space

The gradient flow for $E(\rho)$ in $(\mathcal{P}(\Omega), g_\rho)$ takes the form

$$\partial_t \rho_t = -G(\rho_t)^{-1} \frac{\delta E}{\delta \rho_t}.$$

Here $\frac{\delta E}{\delta \rho_t}$ is the L^2 first variation w.r.t. ρ_t . For example, the Wasserstein gradient flow writes

$$\partial_t \rho_t = -G^W(\rho_t)^{-1} \frac{\delta E}{\delta \rho_t} = \nabla \cdot \left(\rho_t \nabla \frac{\delta E}{\delta \rho_t} \right).$$

We then briefly review Hamiltonian flows in probability space. Given a metric $\mathcal{G}(\rho)$, denote the density function ρ_t as a state variable while function Φ_t as a momentum variable. The Hamiltonian flow in probability space follows

$$\partial_t \begin{bmatrix} \rho_t \\ \Phi_t \end{bmatrix} - \begin{bmatrix} 0 & 1 \\ -1 & 0 \end{bmatrix} \begin{bmatrix} \frac{\delta}{\delta \rho_t} \mathcal{H}(\rho_t, \Phi_t) \\ \frac{\delta}{\delta \Phi_t} \mathcal{H}(\rho_t, \Phi_t) \end{bmatrix} = 0, \quad (2)$$

with respect to the Hamiltonian in density space by $\mathcal{H}(\rho_t, \Phi_t) = \frac{1}{2} \int \Phi_t G(\rho_t)^{-1} \Phi_t dx + E(\rho_t)$. Similar to the Euclidean Hamiltonian function, the Hamiltonian functional in density space consists of a kinetic energy $\frac{1}{2} \int \Phi G(\rho)^{-1} \Phi dx$ and a potential energy $E(\rho)$.

3 Accelerated information gradient flow

We introduce the accelerated gradient flow in probability density space as follows. Let $\alpha_t \geq 0$ be a scalar function of t . We add a damping term $\alpha_t \Phi_t$ to the Hamiltonian flow (2):

$$\partial_t \begin{bmatrix} \rho_t \\ \Phi_t \end{bmatrix} + \begin{bmatrix} 0 \\ \alpha_t \Phi_t \end{bmatrix} - \begin{bmatrix} 0 & 1 \\ -1 & 0 \end{bmatrix} \begin{bmatrix} \frac{\delta}{\delta \rho_t} \mathcal{H}(\rho_t, \Phi_t) \\ \frac{\delta}{\delta \Phi_t} \mathcal{H}(\rho_t, \Phi_t) \end{bmatrix} = 0. \quad (3)$$

We call dynamics (3) *Accelerated Information Gradient (AIG) flow*.

Proposition 1 *The accelerated information gradient flow satisfies*

$$\begin{cases} \partial_t \rho_t - G(\rho_t)^{-1} \Phi_t = 0, \\ \partial_t \Phi_t + \alpha_t \Phi_t + \frac{1}{2} \frac{\delta}{\delta \rho_t} \left(\int \Phi_t G(\rho_t)^{-1} \Phi_t dx \right) + \frac{\delta E}{\delta \rho_t} = 0, \end{cases} \quad (\text{AIG})$$

with initial values $\rho_t|_{t=0} = \rho_0$ and $\Phi_t|_{t=0} = 0$.

We give examples of AIG flows under several metrics, such as Fisher-Rao metric, Wasserstein metric, Kalman-Wasserstein metric and Stein metric. See detailed derivations in the supplementary material.

Example 5 (Fisher-Rao AIG flow)

$$\begin{cases} \partial_t \rho_t - (\Phi_t - \mathbb{E}_{\rho_t}[\Phi_t]) \rho_t = 0, \\ \partial_t \Phi_t + \alpha_t \Phi_t + \frac{1}{2} \Phi_t^2 - \mathbb{E}_{\rho_t}[\Phi_t] \Phi_t + \frac{\delta E}{\delta \rho_t} = 0. \end{cases} \quad (\text{F-AIG})$$

Example 6 (Wasserstein AIG flow, [5, 32])

$$\begin{cases} \partial_t \rho_t + \nabla \cdot (\rho_t \nabla \Phi_t) = 0, \\ \partial_t \Phi_t + \alpha_t \Phi_t + \frac{1}{2} \|\nabla \Phi_t\|^2 + \frac{\delta E}{\delta \rho_t} = 0. \end{cases} \quad (\text{W-AIG})$$

Example 7 (Kalman-Wasserstein AIG flow)

$$\begin{cases} \partial_t \rho_t + \nabla \cdot (\rho_t C^\lambda(\rho_t) \nabla \Phi_t) = 0, \\ \partial_t \Phi_t + \alpha_t \Phi_t + \frac{1}{2} ((x - m(\rho_t))^T B_{\rho_t}(\Phi_t)(x - m(\rho_t)) + \nabla \Phi_t(x)^T C^\lambda(\rho_t) \nabla \Phi_t(x)) + \frac{\delta E}{\delta \rho_t} = 0. \end{cases} \quad (\text{KW-AIG})$$

Here we denote $B_\rho(\Phi) = \int \nabla \Phi \nabla \Phi^T \rho dx$.

Example 8 (Stein AIG flow)

$$\begin{cases} \partial_t \rho_t(x) + \nabla_x \cdot \left(\rho_t(x) \int k(x, y) \rho_t(y) \nabla_y \Phi_t(y) dy \right) = 0, \\ \partial_t \Phi_t(x) + \alpha_t \Phi_t(x) + \int \nabla \Phi_t(x)^T \nabla \Phi_t(y) k(x, y) \rho_t(y) dy + \frac{\delta E}{\delta \rho_t}(x) = 0. \end{cases} \quad (\text{S-AIG})$$

To design fast sampling algorithms, we need to reformulate the evolution of probability in term of samples. In other words, PDEs in term of (ρ, Φ) is the Eulerian formulation in fluid dynamics, while the particle formulation is the flow map equation, known as the Lagrangian formulation. We present examples for W-AIG flow, KW-AIG flow and S-AIG flow, which have particle formulations. We suppose that $X_t \sim \rho_t$ and $V_t = \nabla \Phi_t(X_t)$ are the position and the velocity of a particle at time t .

Example 9 (Particle W-AIG flow) The particle dynamical system for (W-AIG) writes

$$\begin{cases} \frac{d}{dt} X_t = V_t, \\ \frac{d}{dt} V_t = -\alpha_t V_t - \nabla \left(\frac{\delta E}{\delta \rho_t} \right) (X_t). \end{cases} \quad (4)$$

Example 10 (Particle KW-AIG flow) The particle dynamical system for (KW-AIG) writes

$$\begin{cases} \frac{dX_t}{dt} = C^\lambda(\rho_t) V_t, \\ \frac{dV_t}{dt} = -\alpha_t V_t - \mathbb{E}[V_t V_t^T](X_t - \mathbb{E}[X_t]) - \nabla \left(\frac{\delta E}{\delta \rho_t} \right) (X_t). \end{cases} \quad (5)$$

Here the expectation is taken over the particle system.

Example 11 (Particle S-AIG flow) The particle dynamical system for (S-AIG) writes

$$\begin{cases} \frac{dX_t}{dt} = \int k(X_t, y) \nabla \Phi_t(y) \rho_t(y) dy, \\ \frac{dV_t}{dt} = -\alpha_t V_t - \int V_t^T \nabla \Phi_t(y) \nabla_x k(X_t, y) \rho_t(y) dy - \nabla \left(\frac{\delta E}{\delta \rho_t} \right) (X_t). \end{cases} \quad (6)$$

In later on algorithm and convergence analysis, the choice of α_t is important. Similar as the ones in Euclidean space, α_t depends on the convexity of $E(\rho)$ w.r.t. given metrics.

Definition 2 (Convexity in probability space) For a functional $E(\rho)$ defined on the probability space, we say that $E(\rho)$ is β -strongly convex w.r.t. metric g_ρ if there exists a constant $\beta \geq 0$ such that for any $\rho \in \mathcal{P}(\Omega)$ and any $\sigma \in T_\rho \mathcal{P}(\Omega)$, we have

$$g_\rho(\text{Hess } E(\rho) \sigma, \sigma) \geq \beta g_\rho(\sigma, \sigma).$$

Here Hess is the Hessian operator w.r.t. g_ρ . If $\beta = 0$, we say that $E(\rho)$ is convex w.r.t. metric g_ρ .

Again, if $E(\rho)$ is β -strongly convex for $\beta > 0$, then $\alpha_t = 2\sqrt{\beta}$; if $E(\rho)$ is convex, then $\alpha_t = 3/t$.

4 Convergence rate analysis on AIG flows

In this section, we prove the convergence rates of AIG flows under either the Wasserstein metric or the Fisher-Rao metric. This validates the acceleration effect. The proof is motivated by Lyapunov functions of Euclidean accelerated gradient flows in subsection 2.1.

Theorem 1 Suppose that $E(\rho)$ is β -strongly convex for $\beta > 0$. The solution ρ_t to (F-AIG) or (W-AIG) with $\alpha_t = 2\sqrt{\beta}$ satisfies

$$E(\rho_t) \leq C_0 e^{-\sqrt{\beta}t} = \mathcal{O}\left(e^{-\sqrt{\beta}t}\right).$$

If $E(\rho)$ is convex, then the solution ρ_t to (F-AIG) or (W-AIG) with $\alpha_t = 3/t$ satisfies

$$E(\rho_t) \leq C'_0 t^{-2} = \mathcal{O}(t^{-2}).$$

Here the constants C_0, C'_0 only depend on ρ_0 .

Remark 1 For β -strongly convex $E(\rho)$ under the Wasserstein metric, [5] study a compressed Euler equation. They prove similar results with a constant damping coefficient α_t . For convex $E(\rho)$ under the Wasserstein metric, [32] prove similar results with a technical assumption.

5 Discrete-time algorithms for AIG flows

In this section, we present the discrete-time particle implementation of (W-AIG) based on (4). Similar discrete-time algorithms of (KW-AIG) and (S-AIG) are provided in the supplementary material. Here we mainly introduce a kernel bandwidth selection method and an adaptive restart technique to deal with difficulties in numerical implementations.

A typical choice of $E(\rho)$ for sampling is the KL divergence

$$D_{\text{KL}}(\rho \parallel \rho^*) = \int \rho \log \frac{\rho}{e^{-f}} dx - \log Z,$$

where the target density $\rho^*(x) \propto \exp(-f(x))$ and $Z = \int \exp(-f(x)) dx$. Then, (4) is equivalent to

$$\begin{cases} dX_t = V_t dt, \\ dV_t = -\alpha_t V_t dt - \nabla f(X_t) dt - \nabla \log \rho_t(X_t) dt. \end{cases} \quad (7)$$

Consider a particle system $\{X_0^i\}_{i=1}^N$ and let $V_0^i = 0$. In k -th iteration, the update rule follows

$$\begin{cases} X_{k+1}^i = X_k^i + \sqrt{\tau_k} V_{k+1}^i, \\ V_{k+1}^i = \alpha_k V_k^i - \sqrt{\tau_k} (\nabla f(X_k^i) + \xi_k(X_k^i)), \end{cases} \quad (8)$$

for $i = 1, 2, \dots, N$. If $E(\rho)$ is β -strongly convex, then $\alpha_k = \frac{1-\sqrt{\beta\tau_k}}{1+\sqrt{\beta\tau_k}}$; if $E(\rho)$ is convex or β is unknown, then $\alpha_k = \frac{k-1}{k+2}$. Here $\xi_k(x)$ is an approximation of $\nabla \log \rho_k(x)$. For a general distribution, we use the kernel density estimation (KDE) [28], $\tilde{\rho}_k(x) = \frac{1}{N} \sum_{i=1}^N K(x, X_k^i)$ to approximate $\rho_k(x)$. Here $K(x, y)$ is a positive kernel function. Then, ξ_k writes

$$\xi_k(x) = \nabla \log \tilde{\rho}_k(x) = \frac{\sum_{i=1}^N \nabla_x K(x, X_k^i)}{\sum_{i=1}^N K(x, X_k^i)}. \quad (9)$$

A common choice of $K(x, y)$ is a Gaussian kernel with the bandwidth h , $K(x, y) = (2\pi h)^{-n/2} \exp(-\|x - y\|^2/(2h))$. Such approximation can also be found in information-theoretic learning [25] and independent component analysis (ICA) [8].

There are two difficulties in time discretization. For one thing, the bandwidth h strongly affects the estimation of $\nabla \log \rho_t$, so we propose the BM method to learn the bandwidth from Brownian-motion samples. For another, the second equation in (W-AIG) is the Hamilton-Jacobi equation, which usually has strong stiffness. We propose an adaptive restart technique to deal with this problem.

5.1 Learn the bandwidth via Brownian motion

SVGD uses a median (MED) method to choose the bandwidth, i.e.,

$$h_k = \frac{1}{2 \log(N+1)} \text{median} \left(\{\|X_k^i - X_k^j\|^2\}_{i,j=1}^N \right). \quad (10)$$

Liu et al. [14] propose a Heat Equation (HE) method to adaptively adjust bandwidth. Motivated by the HE method, we introduce the Brownian motion (BM) method to adaptively learn the kernel bandwidth based on Brownian-motion samples generated in each iteration.

Given the bandwidth h , $\{X_k^i\}_{i=1}^N$ and a step size s , we can compute two particle systems:

$$Y_k^i(h) = X_k^i - s\xi_k(x; h), \quad Z_k^i = X_k^i + \sqrt{2s}B^i, \quad i = 1, \dots, N$$

where B^i is the standard Brownian motion. Denote the empirical distributions of $\{X_k^i\}_{i=1}^N$, $\{Y_k^i\}_{i=1}^N$ and $\{Z_k^i\}_{i=1}^N$ by $\hat{\rho}_X$, $\hat{\rho}_Y$ and $\hat{\rho}_Z$. With $n \rightarrow \infty$, we shall have $\hat{\rho}_Y = \hat{\rho}_Z = \rho_t|_{t=s}$, where $\hat{\rho}_t$ satisfies $\partial_t \hat{\rho}_t = \Delta \hat{\rho}_t = \nabla \cdot (\hat{\rho}_t \nabla \log \hat{\rho}_t)$ with initial value $\hat{\rho}_t|_{t=0} = \hat{\rho}_X$. With an appropriate bandwidth h , we shall also have $\hat{\rho}_Y = \rho_t|_{t=s}$. Hence, we consider the following optimization problem

$$\min_h \text{MMD}(\hat{\rho}_Y, \hat{\rho}_Z) = \int \int (\hat{\rho}_Y(y) - \hat{\rho}_Z(y))k(y, z)(\hat{\rho}_Y(z) - \hat{\rho}_Z(z))dydz. \quad (11)$$

where MMD (maximum mean discrepancy) evaluates the similarity between $\{Y_k^i\}_{i=1}^N$ and $\{Z_k^i\}_{i=1}^N$. Here, the kernel $k(y, z)$ in MMD is chosen as a Gaussian kernel with bandwidth 1. So we optimize (11) using the bandwidth h_{k-1} from the last iteration as the initialization. For simplicity we denote $\text{BM}(h_{k-1}, \{X_k^i\}_{i=1}^N, s)$ as the minimizer of problem (11). It is the output of the BM method.

5.2 Adaptive restart

To enhance the practical performance, we introduce an adaptive restart technique, which shares the same idea of gradient restart in [24, 35] under the Euclidean case. Consider

$$\varphi_k = - \sum_{i=1}^N \langle V_{k+1}^i, \nabla f(X_k^i) + \xi_k(X_k^i) \rangle, \quad (12)$$

which can be viewed as discrete-time approximation of $-g_{\rho_t}^W(\partial_t \rho_t, G^W(\rho_t)^{-1} \frac{\delta E}{\delta \rho_t}) = -\partial_t E(\rho_t)$. If $\varphi_k < 0$, then we restart the algorithm with initial values $X_0^i = X_k^i$ and $V_0^i = 0$. This essentially keeps $\partial_t E(\rho_t)$ negative along the trajectory. The overall algorithm is summarized below.

Algorithm 1 Discrete-time particle implementation of W-AIG flow

Require: initial positions $\{X_0^i\}_{i=1}^N$, step size τ , number of iteration L .
1: Set $k = 0$, $V_0^i = 0$, $i = 1, \dots, N$. Set the bandwidth h_0 by MED (10).
2: **for** $l = 1, 2, \dots, L$ **do**
3: Compute h_l based on BM method: $h_l = \text{BM}(h_{l-1}, \{X_k^i\}_{i=1}^N, \sqrt{\tau})$.
4: Calculate $\xi_k(X_k^i)$ by (9) with bandwidth h_l .
5: For $i = 1, 2, \dots, N$, update V_{k+1}^i and X_{k+1}^i by (8).
6: Compute φ_k by (12).
7: If $\varphi_k < 0$, set $X_0^i = X_k^i$ and $V_0^i = 0$ and $k = 0$; otherwise set $k = k + 1$.
8: **end for**

6 Numerical experiments

In this section, we present several numerical experiments to demonstrate the acceleration effect of AIG flows, and the strength of adaptive restart technique. Implementation details and additional examples are provided in the supplementary material. Codes can be found in ¹.

6.1 Bayesian logistic regression

We perform the standard Bayesian logistic regression experiment on the Covtype dataset, following the same settings as [16]. Our methods are compared with MCMC, SVGD [16], WNAG [14] and WNeS [13]. SVGD is a gradient descent method based on the Stein metric, which approximates W-GF, see [13, Theorem 2]. WNAG and WNeS are two accelerated methods based on W-GF.

¹<https://github.com/YiifeiWang/Accelerated-Information-Gradient-flow>

We select the kernel bandwidth using either the MED method or the proposed BM method. Figure 1 indicates that the BM method accelerates and stabilizes the performance of GFs and AIGs. The performance of MCMC and WGF are similar and they achieve the best log-likelihood. For a given metric, AIG flows have better test accuracy and test log-likelihood in first 2000 iterations. W-AIG and KW-AIG achieve 75% test accuracy in less than 500 iterations.

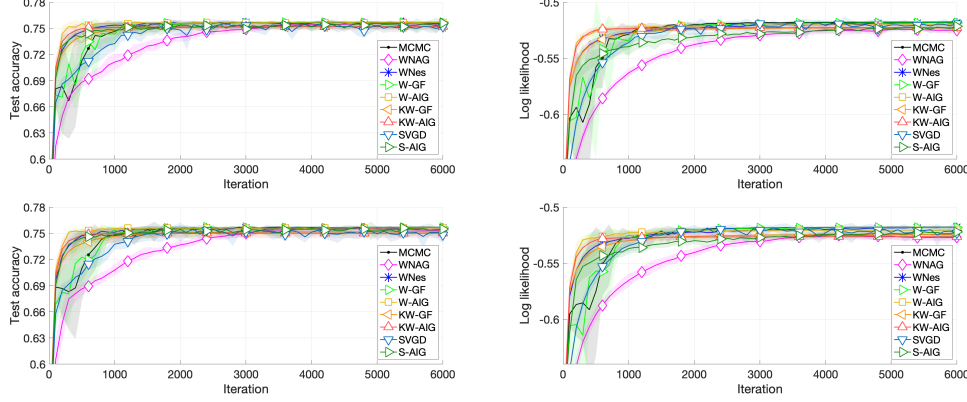


Figure 1: Results on Bayesian logistic regression, averaged over 10 independent trials. The shaded areas show the variance. Top: BM; Bottom: MED. Left: Test accuracy; Right: Test log-likelihood.

6.2 Bayesian neural network

We apply our proposed method on Bayesian neural network over UCI datasets², with the same setting as [34]. We compare W-AIG, W-GF and SVGD. For all methods, we use $N = 10$ particles. The averaged results over 20 independent trials are collected in Table 1. We observe that on most datasets, W-AIG has better test root-mean-square-error and test log-likelihood than W-GF and SVGD. This indicates that W-AIG may have better generalization than W-GF and SVGD.

Dataset	Test RMSE			Test log-likelihood		
	W-AIG	W-GF	SVGD	W-AIG	W-GF	SVGD
Boston	$2.871 \pm 3.41e-3$	$3.077 \pm 5.52e-3$	$2.775 \pm 3.78e-3$	$-2.609 \pm 1.34e-4$	$-2.694 \pm 2.83e-4$	$-2.611 \pm 1.36e-4$
Combined	$4.067 \pm 9.27e-1$	$4.077 \pm 3.85e-4$	$4.070 \pm 2.02e-4$	$-2.822 \pm 5.72e-3$	$-2.825 \pm 2.36e-5$	$-2.823 \pm 1.24e-5$
Concrete	$4.440 \pm 1.34e-1$	$4.883 \pm 1.93e-1$	$4.888 \pm 1.39e-1$	$-2.884 \pm 8.84e-3$	$-2.971 \pm 8.93e-3$	$-2.978 \pm 6.05e-3$
Kin8nm	$0.094 \pm 5.56e-6$	$0.096 \pm 3.36e-5$	$0.095 \pm 1.32e-5$	$0.951 \pm 6.43e-4$	$0.923 \pm 3.37e-3$	$0.932 \pm 1.43e-3$
Wine	$0.606 \pm 1.40e-5$	$0.614 \pm 3.48e-4$	$0.604 \pm 9.89e-5$	$-0.961 \pm 1.28e-4$	$-0.961 \pm 3.17e-4$	$-0.952 \pm 9.89e-5$
Year	$8.876 \pm 3.71e-4$	$8.872 \pm 2.81e-4$	$8.873 \pm 7.19e-4$	$-3.654 \pm 1.00e-5$	$-3.655 \pm 7.82e-6$	$-3.652 \pm 1.28e-5$

Table 1: Test root-mean-square-error (RMSE) and Test log-likelihood.

7 Conclusion

In summary, we propose the framework of AIG flows by damping Hamiltonian flows with respect to certain information metrics in probability space. Theoretically, we establish the convergence rate of F-AIG and W-AIG flows. In algorithm, we propose particle formulations for W-AIG flow, KW-AIG and S-AIG flows. Numerically, we propose discrete-time algorithms and an adaptive restart technique to overcome numerical stiffness of AIG flows. To efficiently approximate $\nabla \log \rho_k(x)$, we introduce a novel kernel selection method by learning from Brownian-motion samples. Numerical experiments verify the acceleration effect of AIG flows and the strength of adaptive restart.

In future works, we intend to systematically explain the stiffness of AIG flows and effects of adaptive restart. We shall apply our results to general information metrics, especially for generalized Wasserstein metrics. We expect to study the related sampling efficient optimization methods and discrete-time algorithms. We also plan to incorporate Hessian operators in probability space [36] in designing higher-order accelerated algorithms. We shall compare these information metrics induced methods in terms of both computational complexity and sampling efficiency.

²<https://archive.ics.uci.edu/ml/datasets.php>

In this appendix, we formulate detailed derivations of examples and proofs of propositions. We also design particle implementations of KW-AIG flows, S-AIG flows and provide detailed implementations of experiments.

A Euler-Lagrange equation, Hamiltonian flows and AIG flows

In this section, we review and derive Euler-Lagrange equation, Hamiltonian flows and Euler-Lagrange formulation of AIG flows in probability space.

A.1 Derivation of the Euler-Lagrange equation

In this subsection, we derive the Euler-Lagrange equation in probability space. For a given metric g_ρ in probability space, we can define a Lagrangian by

$$\mathcal{L}(\rho_t, \partial_t \rho_t) = \frac{1}{2} g_{\rho_t}(\partial_t \rho_t, \partial_t \rho_t) - E(\rho_t).$$

Proposition 2 *The Euler-Lagrange equation for this Lagrangian follows*

$$\partial_t \left(\frac{\delta \mathcal{L}}{\delta(\partial_t \rho_t)} \right) = \frac{\delta \mathcal{L}}{\delta \rho_t} + C(t),$$

where $C(t)$ is a spatially-constant function.

PROOF For a fixed $T > 0$ and two given densities ρ_0, ρ_T , consider the variational problem

$$I(\rho_t) = \inf_{\rho_t} \left\{ \int_0^T \mathcal{L}(\rho_t, \partial_t \rho_t) dt \mid \rho_t|_{t=0} = \rho_0, \rho_t|_{t=T} = \rho_T \right\}.$$

Let $h_t \in \mathcal{F}(\Omega)$ be the smooth perturbation function that satisfies $\int h_t dx = 0, t \in [0, T]$ and $h_t|_{t=0} = h_t|_{t=T} \equiv 0$. Denote $\rho_t^\epsilon = \rho_t + \epsilon h_t$. Note that we have the Taylor expansion

$$\begin{aligned} I(\rho_t^\epsilon) &= \int_0^T \mathcal{L}(\rho_t, \partial_t \rho_t) dt \\ &\quad + \epsilon \int_0^T \int \left(\frac{\delta \mathcal{L}}{\delta \rho_t} h_t + \frac{\delta \mathcal{L}}{\delta(\partial_t \rho_t)} \partial_t h_t \right) dx dt + o(\epsilon). \end{aligned}$$

From $\frac{dI(\rho_t^\epsilon)}{d\epsilon} \Big|_{\epsilon=0} = 0$, it follows that

$$\int_0^T \int \left(\frac{\delta \mathcal{L}}{\delta \rho_t} h_t + \frac{\delta \mathcal{L}}{\delta(\partial_t \rho_t)} \partial_t h_t \right) dx dt = 0.$$

Note that $h_t|_{t=0} = h_t|_{t=T} \equiv 0$. Perform integration by parts w.r.t. t yields

$$\int_0^T \int \left(\frac{\delta \mathcal{L}}{\delta \rho_t} - \partial_t \frac{\delta \mathcal{L}}{\delta(\partial_t \rho_t)} \right) h_t dx dt = 0.$$

Because $\int h_t dx = 0$, the Euler-Lagrange equation holds with a spatially constant function $C(t)$.

A.2 Derivation of Hamiltonian flow

In this subsection, we derive the Hamiltonian flow in the probability space. Denote $\Phi_t = \delta L / \delta(\partial_t \rho_t) = G(\rho_t) \partial_t \rho_t$. Then, the Euler-Lagrange equation can be formulated as a system of (ρ_t, Φ_t) , i.e.,

$$\begin{cases} \partial_t \rho_t - G(\rho_t)^{-1} \Phi_t = 0, \\ \partial_t \Phi_t + \frac{1}{2} \frac{\delta}{\delta \rho_t} \left(\int \Phi_t G(\rho_t)^{-1} \Phi_t dx \right) + \frac{\delta E}{\delta \rho_t} = 0. \end{cases}$$

First, we give a useful identity. Given a metric tensor $G(\rho) : T_\rho \mathcal{P}(\Omega) \rightarrow T_\rho^* \mathcal{P}(\Omega)$, we have

$$\begin{aligned} \int \sigma_1 G(\rho) \sigma_2 dx &= \int G(\rho) \sigma_1 \sigma_2 dx \\ &= \int \Phi_1 G(\rho)^{-1} \Phi_2 dx = \int G(\rho)^{-1} \Phi_1 \Phi_2 dx. \end{aligned} \quad (13)$$

Here $\Phi_1 = G(\rho)^{-1} \sigma_1$ and $\Phi_2 = G(\rho)^{-1} \sigma_2$. We then check that

$$\frac{\delta}{\delta \rho_t} \left(\int \partial_t \rho_t G(\rho_t) \partial_t \rho_t dx \right) = - \frac{\delta}{\delta \rho_t} \left(\int \Phi_t G(\rho_t)^{-1} \Phi_t dx \right). \quad (14)$$

Let $\tilde{\rho}_t = \rho_t + \epsilon h$, where $h \in T_{\rho_t} \mathcal{P}(\Omega)$. For all $\sigma \in T_{\rho_t} \mathcal{P}$, it follows

$$G(\rho_t + \epsilon h)^{-1} G(\rho_t + \epsilon h) \sigma = \sigma.$$

The first-order derivative w.r.t. ϵ of the left hand side shall be 0, i.e.,

$$\left(\frac{\partial G(\rho_t)^{-1}}{\partial \rho_t} \cdot h \right) G(\rho_t) \sigma + G(\rho_t)^{-1} \left(\frac{\partial G(\rho_t)}{\partial \rho_t} \cdot h \right) \sigma = 0.$$

Because $\partial_t \rho_t = G(\rho)^{-1} \Phi_t$, applying (13) yields

$$\begin{aligned} \int \partial_t \rho_t \left(\frac{\partial G(\rho_t)}{\partial \rho_t} \cdot h \right) \partial_t \rho_t dx &= \int \Phi_t G(\rho_t)^{-1} \left(\frac{\partial G(\rho_t)}{\partial \rho_t} \cdot h \right) \partial_t \rho_t dx \\ &= - \int \Phi_t \left(\frac{\partial G(\rho_t)^{-1}}{\partial \rho_t} \cdot h \right) G(\rho_t) \partial_t \rho_t dx = - \int \Phi_t \left(\frac{\partial G(\rho_t)^{-1}}{\partial \rho_t} \cdot h \right) \Phi_t dx. \end{aligned} \quad (15)$$

Based on basic calculations, we can compute that

$$\int \partial_t \rho_t G(\tilde{\rho}_t) \partial_t \rho_t dx - \int \partial_t \rho_t G(\rho_t) \partial_t \rho_t dx = \epsilon \int \partial_t \rho_t \left(\frac{\partial G(\rho_t)}{\partial \rho_t} \cdot h \right) \partial_t \rho_t dx + o(\epsilon), \quad (16)$$

$$- \int \Phi_t G(\tilde{\rho}_t)^{-1} \Phi_t dx + \int \Phi_t G(\rho_t)^{-1} \Phi_t dx = -\epsilon \int \Phi_t \left(\frac{\partial G(\rho_t)^{-1}}{\partial \rho_t} \cdot h \right) \Phi_t dx + o(\epsilon). \quad (17)$$

Combining (15), (16) and (17) yields (14). Hence, the Euler-Lagrange equation is equivalent to

$$\partial_t \Phi_t = \frac{1}{2} \frac{\delta}{\delta \rho_t} \left(\int \partial_t \rho_t G(\rho_t) \partial_t \rho_t dx \right) - \frac{\delta E}{\delta \rho_t} = - \frac{1}{2} \frac{\delta}{\delta \rho_t} \left(\int \Phi_t G(\rho_t)^{-1} \Phi_t dx \right) - \frac{\delta E}{\delta \rho_t}.$$

This equation combining with $\partial_t \rho_t = G(\rho)^{-1} \Phi_t$ recovers the Hamiltonian flow. In short, the Euler-Lagrange equation is from the primal coordinates $(\rho_t, \partial_t \rho_t)$ and the Hamiltonian flow is from the dual coordinates (ρ_t, Φ_t) . Similar interpretations can be found in [7].

A.3 The Euler-Lagrangian formulation of AIG flows

We can formulate the AIG flow as a second-order equation of ρ_t ,

$$\frac{D^2}{Dt^2} \rho_t + \alpha_t \partial_t \rho_t + G(\rho_t)^{-1} \frac{\delta E}{\delta \rho_t} = 0.$$

Here D^2/Dt^2 is the covariant derivative w.r.t. metric $G(\rho)$. We can also explicitly write $\frac{D^2}{Dt^2} \rho_t$ as

$$\frac{D^2}{Dt^2} \rho_t = \partial_{tt} \rho_t - (\partial_t G(\rho_t)^{-1}) \partial_t \rho_t + \frac{1}{2} G(\rho_t)^{-1} \frac{\delta}{\delta \rho_t} \left(\int \partial_t \rho_t G(\rho_t) \partial_t \rho_t dx \right).$$

B Derivation of examples in Section 3

In this section, we present examples of gradient flows, Hamiltonian flows and derive particle dynamics examples in Section 3.

B.1 Examples of gradient flows

We first present several examples of gradient flows w.r.t. different metrics.

Example 12 (Fisher-Rao gradient flow)

$$\partial_t \rho_t = -G^F(\rho_t)^{-1} \frac{\delta E}{\delta \rho_t} = -\rho_t \left(\frac{\delta E}{\delta \rho_t} - \int \frac{\delta E}{\delta \rho_t} \rho_t dy \right).$$

Example 13 (Wasserstein gradient flow)

$$\partial_t \rho_t = -G^W(\rho_t)^{-1} \frac{\delta E}{\delta \rho_t} = \nabla \cdot \left(\rho_t \nabla \frac{\delta E}{\delta \rho_t} \right).$$

Example 14 (Kalman-Wasserstein gradient flow)

$$\partial_t \rho_t = -G^{KW}(\rho_t)^{-1} \frac{\delta E}{\delta \rho_t} = \nabla \cdot \left(\rho_t C^\lambda(\rho_t) \nabla \left(\frac{\delta E}{\delta \rho_t} \right) \right).$$

Example 15 (Stein gradient flow)

$$\partial_t \rho_t = -G^S(\rho_t)^{-1} \frac{\delta E}{\delta \rho_t} = \nabla_x \cdot \left(\rho_t(x) \int k(x, y) \rho_t(y) \nabla_y \left(\frac{\delta E}{\delta \rho_t} \right) dy \right).$$

B.2 Examples of Hamiltonian flows

We next present several examples of Hamiltonian flows w.r.t. different metrics.

Example 16 (Fisher-Rao Hamiltonian flow) The Fisher-Rao Hamiltonian flow follows

$$\begin{cases} \partial_t \rho_t - \rho_t (\Phi_t - \mathbb{E}_{\rho_t}[\Phi_t]) = 0, \\ \partial_t \Phi_t + \frac{1}{2} \Phi_t^2 - \mathbb{E}_{\rho_t}[\Phi_t] \Phi_t + \frac{\delta E}{\delta \rho_t} = 0, \end{cases}$$

where the corresponding Hamiltonian is

$$\mathcal{H}^F(\rho_t, \Phi_t) = \frac{1}{2} \left(\mathbb{E}_{\rho_t}[\Phi_t^2] - (\mathbb{E}_{\rho_t}[\Phi_t])^2 \right) + E(\rho_t).$$

Example 17 (Wasserstein Hamiltonian flow) The Wasserstein Hamiltonian flow writes

$$\begin{cases} \partial_t \rho_t + \nabla \cdot (\rho_t \nabla \Phi_t) = 0, \\ \partial_t \Phi_t + \frac{1}{2} \|\nabla \Phi_t\|^2 + \frac{\delta E}{\delta \rho_t} = 0, \end{cases}$$

where the corresponding Hamiltonian is

$$\mathcal{H}^W(\rho_t, \Phi_t) = \frac{1}{2} \int \|\nabla \Phi_t\|^2 \rho_t dx + E(\rho_t).$$

This is identical to the Wasserstein Hamiltonian flow introduced in [7].

Example 18 (Kalman-Wasserstein Hamiltonian flow) The Kalman-Wasserstein Hamiltonian flow writes

$$\begin{cases} \partial_t \rho_t + \nabla \cdot (\rho_t C^\lambda(\rho_t) \nabla \Phi_t) = 0, \\ \partial_t \Phi_t + \frac{1}{2} ((x - m(\rho_t))^T B_{\rho_t}(\Phi_t)(x - m(\rho_t)) + \nabla \Phi_t(x)^T C^\lambda(\rho_t) \nabla \Phi_t(x)) + \frac{\delta E}{\delta \rho_t} = 0, \end{cases}$$

where the corresponding Hamiltonian is

$$\mathcal{H}^{KW}(\rho_t, \Phi_t) = \frac{1}{2} \int \nabla \Phi_t^T C^\lambda(\rho_t) \nabla \Phi_t \rho_t dx + E(\rho_t).$$

Example 19 (Stein Hamiltonian flow) The Stein Hamiltonian flow writes

$$\begin{cases} \partial_t \rho_t(x) = -\nabla_x \cdot \left(\rho_t(x) \int k(x, y) \rho_t(y) \nabla_y \Phi_t(y) dy \right), \\ \partial_t \Phi_t(x) = -\int \nabla \Phi_t(x)^T \nabla \Phi_t(y) k(x, y) \rho_t(y) dy - \frac{\delta E}{\delta \rho_t}(x), \end{cases}$$

where the corresponding Hamiltonian is

$$\mathcal{H}(\rho_t, \Phi_t) = \frac{1}{2} \int \int \nabla \Phi_t(x)^T \nabla \Phi_t(y) k(x, y) \rho_t(x) \rho_t(y) dx dy + E(\rho_t).$$

B.3 The derivation of Example 9 (Wasserstein metric) in Section 3

We start with an identity. For a twice differentiable $\Phi(x)$, we have

$$\frac{1}{2} \nabla \|\nabla \Phi\|^2 = \nabla^2 \Phi \nabla \Phi = (\nabla \Phi \cdot \nabla) \nabla \Phi. \quad (18)$$

From (W-AIG), it follows that

$$\partial_t \rho_t + \nabla \cdot (\rho_t \nabla \Phi_t) = 0. \quad (19)$$

This is the continuity equation of ρ_t . Hence, on the particle level, X_t shall follows

$$dX_t = \nabla \Phi_t(X_t) dt.$$

Let $V_t = \nabla \Phi_t(X_t)$. Then, by the material derivative in fluid dynamics and (W-AIG), we have

$$\begin{aligned} \frac{dV_t}{dt} &= \frac{d}{dt} \nabla \Phi_t(X_t) = (\partial_t + \nabla \Phi_t(X_t) \cdot \nabla) \nabla \Phi_t(X_t) dt \\ &= \left(-\alpha_t \nabla \Phi_t(X_t) - \frac{1}{2} \nabla \|\nabla \Phi\|^2 - \nabla \frac{\delta E}{\delta \rho_t} \right) dt + (\nabla \Phi \cdot \nabla) \nabla \Phi dt \\ &= -\alpha_t \nabla \Phi_t(X_t) dt - \nabla \frac{\delta E}{\delta \rho_t}(X_t) dt = -\alpha_t V_t dt - \nabla \frac{\delta E}{\delta \rho_t}(X_t) dt. \end{aligned}$$

B.4 The derivations of Example 7 and 10 (Kalman-Wasserstein metric) in Section 3

We first derive the Hamiltonian flow under the Kalman-Wasserstein metric. We first show that

$$\frac{\delta}{\delta \rho} \left\{ \int \Phi G^{KW}(\rho)^{-1} \Phi dx \right\} = (x - m(\rho))^T B_\rho(\Phi)(x - m(\rho)) + \nabla \Phi(x)^T C^\lambda(\rho) \nabla \Phi(x). \quad (20)$$

From the definition of Kalman-Wasserstein metric, we have

$$\begin{aligned} \int \Phi G^{KW}(\rho)^{-1} \Phi dx &= \int \nabla \Phi^T C^\lambda(\rho) \nabla \Phi \rho dx \\ &= \left\langle C^\lambda(\rho), \int \nabla \Phi^T \nabla \Phi \rho dx \right\rangle = \langle C^\lambda(\rho), B_\rho(\Phi) \rangle. \end{aligned}$$

Let $\hat{\rho} = \rho + \epsilon h$, where $h \in T_\rho \mathcal{P}(\Omega)$. Then, we can compute that

$$\begin{aligned} &\langle C^\lambda(\rho + \epsilon h), B_{\rho + \epsilon h}(\Phi) \rangle - \langle C^\lambda(\rho), B_\rho(\Phi) \rangle \\ &= \langle C^\lambda(\rho + \epsilon h) - C^\lambda(\rho), B_\rho(\Phi) \rangle + \langle C^\lambda(\rho), B_{\rho + \epsilon h}(\Phi) - B_\rho(\Phi) \rangle. \end{aligned}$$

We note that

$$\begin{aligned} &C^\lambda(\rho + \epsilon h) - C^\lambda(\rho) \\ &= \epsilon \int m(h)(x - m(\rho))^T \rho dx + \epsilon \int (x - m(\rho))m(h)^T \rho dx \\ &\quad + \epsilon \int (x - m(\rho))(x - m(\rho))^T h dx + O(\epsilon^2) \\ &= \epsilon \int (x - m(\rho))(x - m(\rho))^T h dx + O(\epsilon^2). \\ &B_{\rho + \epsilon h}(\Phi) - B_\rho(\Phi) = \epsilon \int h \nabla \Phi \nabla \Phi^T dx. \end{aligned}$$

Hence, we can derive

$$\begin{aligned} &\langle C^\lambda(\rho + \epsilon h), B_{\rho + \epsilon h}(\Phi) \rangle - \langle C^\lambda(\rho), B_\rho(\Phi) \rangle \\ &= \epsilon \int h \langle \nabla \Phi \nabla \Phi^T, C(\rho) \rangle dx + \epsilon \int h \langle (x - m(\rho))(x - m(\rho))^T, B_\rho(\Phi) \rangle dx + O(\epsilon^2). \end{aligned}$$

This proves (20). Hence, the Hamiltonian flow under the Kalman-Wasserstein metric follows

$$\begin{cases} \partial_t \rho_t + \nabla \cdot (\rho_t C^\lambda(\rho_t) \nabla \Phi_t) = 0, \\ \partial_t \Phi_t + \frac{1}{2} ((x - m(\rho_t))^T B_{\rho_t}(\Phi_t)(x - m(\rho_t)) + \nabla \Phi_t(x)^T C^\lambda(\rho_t) \nabla \Phi_t(x)) + \frac{\delta E}{\delta \rho_t} = 0. \end{cases} \quad (21)$$

Adding a linear damping term $\alpha_t \Phi_t$ to the second equation in (21) yields Example 7.
For Example 10, suppose that X_t follows ρ_t and $V_t = \nabla \Phi_t(X_t)$. Then, we shall have

$$\frac{d}{dt} X_t = C^\lambda(\rho_t) V_t,$$

Note that $V_t = \nabla \Phi_t(X_t)$, we can establish that

$$\begin{aligned} \frac{d}{dt} V_t &= (\partial_t + (C^\lambda(\rho_t) \nabla \Phi_t \cdot \nabla) \nabla \Phi_t(X_t)) \\ &= \nabla \partial_t \Phi_t(X_t) + \nabla^2 \Phi_t(X_t) C^\lambda(\rho_t) \nabla \Phi_t(X_t). \end{aligned}$$

The last inequality can be established as follows. For $i = 1, \dots, d$, we have

$$\begin{aligned} (C^\lambda(\rho_t) \nabla \Phi_t \cdot \nabla) \nabla_i \Phi_t(X_t) &= \sum_{j=1}^d (C^\lambda(\rho_t) \nabla \Phi_t)_j \nabla_j \nabla_i \Phi_t(X_t) \\ &= \sum_{j=1}^d \nabla_{ij} \Phi_t(X_t) (C^\lambda(\rho_t) \nabla \Phi_t)_j = (\nabla^2 \Phi_t C^\lambda(\rho_t) \nabla \Phi_t)_i. \end{aligned}$$

According to the chain rule, we also have

$$\nabla(\nabla \Phi_t(x)^T C^\lambda(\rho_t) \nabla \Phi_t(x)) = 2 \nabla^2 \Phi_t(x) C^\lambda(\rho_t) \nabla \Phi_t(x)$$

As a result, we can establish that

$$\begin{aligned} \frac{d}{dt} V_t &= -\alpha_t V_t - B_{\rho_t}(\Phi_t)(X_t - M(\rho_t)) - \nabla \delta_{\rho_t} E \\ &= -\alpha_t V_t - \mathbb{E}[V_t V_t^T](X_t - \mathbb{E}[X_t]) - \nabla \delta_{\rho_t} E. \end{aligned} \tag{22}$$

In summary, the KW-AIG flow in the particle formulation writes

$$\begin{cases} \frac{d}{dt} X_t = \mathbb{E}[(X_t - \mathbb{E}[X_t])(X_t - \mathbb{E}[X_t])^T] V_t, \\ \frac{d}{dt} V_t = -\alpha_t V_t - \mathbb{E}[V_t V_t^T](X_t - \mathbb{E}[X_t]) - \nabla \delta_{\rho_t} E. \end{cases} \tag{23}$$

B.5 The derivations of Example 8 and 11 (Stein metric) in Section 3

For an objective function $E(\rho)$, the Hamiltonian follows

$$\mathcal{H}(\rho, \Phi) = \frac{1}{2} \int \int \nabla \Phi(x)^T \nabla \Phi(y) k(x, y) \rho(x) \rho(y) dx dy + E(\rho).$$

We note that

$$\begin{aligned} \frac{\delta}{\delta \rho} \left[\frac{1}{2} \int \int \nabla \Phi(x)^T \nabla \Phi(y) k(x, y) \rho(x) \rho(y) dx dy \right] (x) \\ = \int \nabla \Phi(x)^T \nabla \Phi(y) k(x, y) \rho(y) dy. \end{aligned}$$

Hence, the Hamiltonian flow writes

$$\begin{cases} \partial_t \rho_t(x) = -\nabla_x \cdot \left(\rho_t(x) \int k(x, y) \rho_t(y) \nabla_y \Phi_t(y) dy \right), \\ \partial_t \Phi_t(x) = - \int \nabla \Phi_t(x)^T \nabla \Phi_t(y) k(x, y) \rho_t(y) dy - \frac{\delta E}{\delta \rho_t}(x). \end{cases} \tag{24}$$

Adding a linear damping term $\alpha_t \Phi_t$ to the second equation in (24) yields Example 8.

For Example 11, similarly, suppose that X_t follows ρ_t and $V_t = \nabla \Phi_t(X_t)$. Then, we shall have

$$\frac{d}{dt} X_t = \int k(X_t, y) \nabla \Phi_t(y) \rho_t(y) dy.$$

We note that

$$\begin{aligned} & \nabla \left(\int \nabla \Phi(x)^T \nabla \Phi(y) k(x, y) \rho(y) dy \right) \\ &= \nabla^2 \Phi(x) \int \nabla \Phi(y) k(x, y) \rho(y) dy + \int \nabla \Phi(x)^T \nabla \Phi(y) \nabla_x k(x, y) \rho(y) dy. \end{aligned}$$

Hence, we have

$$\begin{aligned} \frac{d}{dt} V_t &= \partial_t \nabla \Phi_t(X_t) + \nabla^2 \Phi_t(X_t) \left(\int k(x, y) \rho_t(y) \nabla_y \Phi_t(y) dy \right) \\ &= -\alpha_t \nabla \Phi_t(X_t) - \int \nabla \Phi_t(X_t)^T \nabla \Phi_t(y) \nabla_x k(X_t, y) \rho(y) dy - \nabla \left(\frac{\delta E}{\delta \rho_t} \right) (X_t) \\ &= -\alpha_t V_t - \int V_t^T \nabla \Phi_t(y) \nabla_x k(X_t, y) \rho(y) dy - \nabla \left(\frac{\delta E}{\delta \rho_t} \right) (X_t). \end{aligned}$$

This derives Example 11.

C Proof of convergence rate under Wasserstein metric

In this section, we briefly review the Riemannian structure of probability space and present proofs of propositions in Section 4 under Wasserstein metric.

C.1 A brief review on the geometric properties of the probability space

Suppose that we have a metric g_ρ in probability space $\mathcal{P}(\Omega)$. Given two probability densities $\rho_0, \rho_1 \in \mathcal{P}(\Omega)$, we define the distance as follows

$$\mathcal{D}(\rho_0, \rho_1)^2 = \inf_{\hat{\rho}_s} \left\{ \int_0^1 g_{\hat{\rho}_s}(\partial_s \hat{\rho}_s, \partial_s \hat{\rho}_s) ds : \hat{\rho}_s|_{s=0} = \rho_0, \hat{\rho}_s|_{s=1} = \rho_1 \right\}.$$

The minimizer $\hat{\rho}_s$ of the above problem is defined as the geodesic curve connecting ρ_0 and ρ_1 . An exponential map at $\rho_0 \in \mathcal{P}(\Omega)$ is a mapping from the tangent space $T_{\rho_0} \mathcal{P}(\Omega)$ to $\mathcal{P}(\Omega)$. Namely, $\sigma \in T_{\rho_0} \mathcal{P}(\Omega)$ is mapped to a point $\rho_1 \in \mathcal{P}(\Omega)$ such that there exists a geodesic curve $\hat{\rho}_s$ satisfying $\hat{\rho}_s|_{s=0} = \rho_0$, $\partial_s \hat{\rho}_s|_{s=0} = \sigma$, and $\hat{\rho}_s|_{s=1} = \rho_1$.

C.2 The inverse of exponential map

In this subsection, we characterize the inverse of exponential map in the probability space with the Wasserstein metric.

Proposition 3 Denote the geodesic curve $\gamma(s)$ that connects ρ_t and ρ^* by $\gamma(s) = (sT_t + (1-s)\text{Id}) \# \rho_t$, $s \in [0, 1]$. Here Id is the identity mapping from \mathbb{R}^n to itself. Then, $\partial_s \gamma(s)|_{s=0}$ corresponds to a tangent vector $-\nabla \cdot (\rho_t(x)(T_t(x) - x)) \in T_{\rho_t} \mathcal{P}(\Omega)$.

For simplicity, we denote $T_t^s = (sT_t + (1-s)\text{Id})^{-1}$, $s \in [0, 1]$. Based on the theory of optimal transport [33], we can write the explicit formula of the geodesic curve $\gamma(s)$ by

$$\gamma(s) = T_t^s \# \rho_t = \det(\nabla T_t^s) \rho_t \circ T_t^s.$$

Through basic calculations, we can compute that

$$\begin{aligned} \frac{d}{ds} T_t^s \Big|_{s=0} &= - \frac{d}{ds} (sT_t + (1-s)\text{Id}) \Big|_{s=0} = \text{Id} - T_t. \\ \frac{d}{ds} \det(\nabla T_t^s) \Big|_{s=0} &= \frac{d}{ds} \det(I + s(I - DT_t) + o(s)) \Big|_{s=0} \\ &= \text{tr}(I - DT_t). \end{aligned}$$

Therefore, we have

$$\begin{aligned} & \partial_s \gamma(s)|_{s=0}(x) \\ &= \text{tr}(I - \nabla T_t) \rho_t(x) + \langle \nabla \rho_t(x), x - \varphi_t(x) \rangle \\ &= \nabla \cdot (x - T_t(x)) \rho_t(x) + \langle \nabla \rho_t(x), x - T_t(x) \rangle \\ &= -\nabla \cdot (\rho_t(x)(T_t(x) - x)), \end{aligned}$$

which completes the proof.

C.3 Sketch of proof

In Euclidean case, the convergence rate of accelerated gradient flow is based on the construction of Lyapunov functions. Namely, for β -strongly convex $f(x)$, consider a Lyapunov function:

$$\mathcal{E}(t) = \frac{e^{\sqrt{\beta}t}}{2} \|\sqrt{\beta}(x_t - x^*) + \dot{x}_t\|^2 + e^{\sqrt{\beta}t}(f(x_t) - f(x^*)).$$

For general convex $f(x)$, consider a Lyapunov function

$$\mathcal{E}(t) = \frac{1}{2} \left\| (x_t - x^*) + \frac{t}{2} \dot{x}_t \right\|^2 + \frac{t^2}{4} (f(x_t) - f(x^*)).$$

Based on different assumptions on the convexity of $f(x)$, we can prove that these Lyapunov function are not increasing w.r.t. t . Hence, the convergence rates are obtained.

Following Lyapunov functions in Euclidean space, we provide a sketch in the proof of Theorem 1. We first consider the case where $E(\rho)$ is β -strongly convex for $\beta > 0$. Let T_t denote the optimal transport plan from ρ_t to ρ^* . Consider a Lyapunov function

$$\begin{aligned} \mathcal{E}(t) = & \frac{e^{\sqrt{\beta}t}}{2} \int \left\| -\sqrt{\beta}(T_t(x) - x) + \nabla \Phi_t(x) \right\|^2 \rho_t(x) dx \\ & + e^{\sqrt{\beta}t} (E(\rho_t) - E(\rho^*)). \end{aligned} \quad (25)$$

Here the $-(T_t(x) - x)$ term can be viewed as $x_t - x^*$ and $\nabla \Phi_t$ can be viewed as \dot{x}_t . Different from the Euclidean case, we introduce an important lemma in proving that $\mathcal{E}(t)$ is non-increasing.

Lemma 1 Denote $u_t = \partial_t(T_t)^{-1} \circ T_t$. Then, u_t satisfies

$$\nabla \cdot (\rho_t(u_t - \nabla \Phi_t)) = 0.$$

We also have

$$\partial_t T_t(x) = -\nabla T_t(x) u_t(x).$$

More importantly, we have

$$\begin{aligned} \int \langle \nabla \Phi_t - u_t, \nabla T_t \nabla \Phi_t \rangle \rho_t dx &\geq 0, \\ \int \langle \nabla \Phi_t - u_t, \nabla T_t(x) (T_t(x) - x) \rangle \rho_t &= 0. \end{aligned}$$

We then demonstrate that $\mathcal{E}(t)$ is not increasing w.r.t. t .

Proposition 4 Suppose that $E(\rho)$ satisfies $\text{Hess}(\beta)$ for $\beta > 0$. ρ_t is the solution to (W-AIG) with $\alpha_t = 2\sqrt{\beta}$. Then, $\mathcal{E}(t)$ defined in (25) satisfies $\dot{\mathcal{E}}(t) \leq 0$. As a result,

$$E(\rho_t) \leq e^{-\sqrt{\beta}t} \mathcal{E}(t) \leq e^{-\sqrt{\beta}t} \mathcal{E}(0) = \mathcal{O}(e^{-\sqrt{\beta}t}).$$

Note that $\mathcal{E}(0)$ only depends on ρ_0 . This proves the first part of Theorem 1.

We now focus on the case where $E(\rho)$ is convex. Similarly, we construct the following Lyapunov function.

$$\begin{aligned} \mathcal{E}(t) = & \frac{1}{2} \int \left\| -(T_t(x) - x) + \frac{t}{2} \nabla \Phi_t(x) \right\|^2 \rho_t(x) dx \\ & + \frac{t^2}{4} (E(\rho_t) - E(\rho^*)). \end{aligned} \quad (26)$$

Proposition 5 Suppose that $E(\rho)$ satisfies $\text{Hess}(0)$. ρ_t is the solution to (W-AIG) with $\alpha_t = 3/t$. Then, $\mathcal{E}(t)$ defined in (26) satisfies $\dot{\mathcal{E}}(t) \leq 0$. As a result,

$$E(\rho_t) \leq \frac{4}{t^2} \mathcal{E}(t) \leq \frac{4}{t^2} \mathcal{E}(0) = \mathcal{O}(t^{-2}).$$

Because $\mathcal{E}(0)$ only depends on ρ_0 , we complete the proof.

C.4 The proof of Proposition 4 and 5

The main goal of this subsection is to prove the Lyapunov function $\mathcal{E}(t)$ is non-increasing.

Preparations. We first give a better characterization of the optimal transport plan T_t . We can write $T_t = \nabla \Psi_t$, where Ψ_t is a strictly convex function, see [33]. This indicates that ∇T_t is symmetric. We then introduce the following proposition.

Proposition 6 *Suppose that $E(\rho)$ satisfies Hess(β) for $\beta \geq 0$. Let $T_t(x)$ be the optimal transport plan from ρ_t to ρ^* , then*

$$E(\rho^*) \geq E(\rho_t) + \int \left\langle T_t(x) - x, \nabla \frac{\delta E}{\delta \rho_t} \right\rangle \rho dx + \frac{\beta}{2} \int \|T_t(x) - x\|^2 \rho_t dx.$$

This is a direct result of β -displacement convexity of $E(\rho)$ based on Proposition 3.

Lemma 2 *Denote $u_t = \partial_t(T_t)^{-1} \circ T_t$. Then, u_t satisfies*

$$\nabla \cdot (\rho_t(u_t - \nabla \Phi_t)) = 0. \quad (27)$$

We also have

$$\partial_t T_t(x) = -\nabla T_t(x) u_t(x). \quad (28)$$

PROOF Because $(T_t)^{-1} \# \rho^* = \rho_t$, let $u_t = \partial_t(T_t)^{-1} \circ T_t$ and $X_t = (T_t)^{-1} X_0$, where $X_0 \sim \rho^*$. This yields $\frac{d}{dt} X_t = u_t(X_t)$. The distribution of X_t follows ρ_t . By the Euler's equation, ρ_t shall follow

$$\partial_t \rho_t + \nabla \cdot (\rho_t u_t) = 0.$$

Combining this with the continuity equation (19) yields (27).

Then, we formulate $\partial_t T_t(x)$ with u_t . By the Taylor expansion,

$$T_{t+s}(x) = T_t(x) + s \partial_t T_t(x) + o(s).$$

Let $y = (T_t)^{-1} x$. it follows

$$(T_{t+s})^{-1}(x) = (T_t)^{-1}(x) + s u_t((T_t)^{-1}(x)) + o(s) = y + s u_t(y) + o(s).$$

Therefore, we have

$$\begin{aligned} 0 &= T_{t+s}((T_{t+s})^{-1}(x)) - x \\ &= T_{t+s}(y + s u_t(y) + o(s)) - x \\ &= T_t(y + s u_t(y)) + s \partial_t T_t(y + s u_t(y)) - x + o(s) \\ &= T_t(y) + s \nabla T_t(y) u_t(y) + s \partial_t T_t(y) - x + o(s) \\ &= s [\nabla T_t(y) u_t(y) + \partial_t T_t(y)] + o(s). \end{aligned}$$

We shall have $\nabla T_t(y) u_t(y) + \partial_t T_t(y) = 0$. Replacing y by x yields (28).

The following lemma illustrates two important properties of u_t and $\partial_t T_t$.

Lemma 3 *For u_t satisfying (27), we have*

$$\begin{aligned} \int \langle \nabla \Phi_t - u_t, \nabla T_t \nabla \Phi_t \rangle \rho_t dx &\geq 0, \\ \int \langle \nabla \Phi_t - u_t, \nabla T_t(x) (T_t(x) - x) \rangle \rho_t &= 0. \end{aligned}$$

PROOF We first notice that $u_t - \nabla \Phi_t$ is divergence-free in term of ρ_t . From $-\nabla T_t u_t = \partial_t T_t = \nabla \partial_t \Psi_t$, we observe that $-\nabla T_t u_t$ is the gradient of $\partial_t \Psi_t$. Therefore,

$$\int \langle \nabla \Phi_t - u_t, \nabla T_t u_t \rangle \rho_t = - \int \langle \partial_t \Psi_t, \nabla \cdot (\rho_t (\nabla \Phi_t - u_t)) \rangle = 0.$$

Based on our previous characterization on the optimal transport plan T_t , $\nabla T_t = \nabla^2 \Psi_t$ is symmetric positive definite. This yields that

$$\begin{aligned} &\int \langle \nabla \Phi_t - u_t, \nabla T_t \nabla \Phi_t \rangle \rho_t dx \\ &= \int \langle \nabla \Phi_t - u_t, \nabla T_t \nabla \Phi_t \rangle \rho_t dx - \int \langle \nabla \Phi_t - u_t, \nabla T_t u_t \rangle \rho_t \\ &= \int \langle \nabla \Phi_t - u_t, \nabla T_t (\nabla \Phi_t - u_t) \rangle \rho_t dx \geq 0. \end{aligned}$$

The last inequality utilizes that ∇T_t is positive definite and ρ_t is non-negative. Then, we prove the equality in Lemma 3. Because $\nabla T_t(x)(T_t(x) - x) = \frac{1}{2}\nabla(\|T_t(x) - x\|^2 + T_t(x) - \|x\|^2)$ is a gradient. Similarly, it follows

$$\int \langle \nabla \Phi_t - u_t, \nabla T_t(x)(T_t(x) - x) \rangle \rho_t = 0.$$

Lemma 3 and the relationship (28) gives

$$-\int \langle \partial_t T_t, \nabla \Phi_t \rangle \rho_t dx = \int \langle u_t, \nabla T_t \nabla \Phi_t \rangle \rho_t dx \leq \int \langle \nabla \Phi_t, \nabla T_t \nabla \Phi_t \rangle \rho_t dx, \quad (29)$$

$$\int \langle \partial_t T_t, T_t(x) - x \rangle \rho_t dx = - \int \langle \nabla \Phi_t, \nabla T_t(x)(T_t(x) - x) \rangle \rho_t dx. \quad (30)$$

Proof of Proposition 4. Based on the definition of the Wasserstein metric, we have

$$\partial_t E(\rho_t) = - \int \frac{\delta E}{\delta \rho_t} \nabla \cdot (\rho_t \nabla \Phi_t) dx.$$

Differentiating $\mathcal{E}(t)$ w.r.t. t renders

$$\begin{aligned} & \dot{\mathcal{E}}(t) e^{-\sqrt{\beta}t} \\ &= \beta \int \langle \partial_t T_t, T_t(x) - x \rangle \rho_t dx - \frac{\beta}{2} \int \|T_t(x) - x\|^2 \nabla \cdot (\rho_t \nabla \Phi_t) dx \\ & \quad - \sqrt{\beta} \int \langle \partial_t T_t, \nabla \Phi_t \rangle \rho_t dx - \sqrt{\beta} \int \langle T_t(x) - x, \partial_t \nabla \Phi_t \rangle \rho_t dx \\ & \quad + \sqrt{\beta} \int \langle T_t(x) - x, \nabla \Phi_t \rangle \nabla \cdot (\rho_t \nabla \Phi_t) dx + \int \langle \nabla \Phi_t, \partial_t \nabla \Phi_t \rangle \rho_t dx \\ & \quad - \frac{1}{2} \int \|\nabla \Phi_t\|^2 \nabla \cdot (\rho_t \nabla \Phi_t) - \int \frac{\delta E}{\delta \rho_t} \nabla \cdot (\rho_t \nabla \Phi_t) dx \\ & \quad + \frac{\sqrt{\beta}}{2} \int \|\nabla \Phi_t\|^2 \rho_t dx - \beta \int \langle T_t(x) - x, \nabla \Phi_t(x) \rangle \rho_t dx \\ & \quad + \frac{\sqrt{\beta^3}}{2} \int \|T_t(x) - x\|^2 \rho_t dx + \sqrt{\beta}(E(\rho_t) - E(\rho^*)). \end{aligned} \quad (31)$$

For the part (31), Proposition 6 renders

$$\begin{aligned} & \frac{\sqrt{\beta^3}}{2} \int \|T_t(x) - x\|^2 \rho_t dx + \sqrt{\beta} E(\rho_t) \\ & \leq - \sqrt{\beta} \int \left\langle T_t(x) - x, \nabla \frac{\delta E}{\delta \rho_t} \right\rangle \rho_t dx. \end{aligned} \quad (32)$$

We first compute the terms with the coefficient β^0 in $\dot{\mathcal{E}}(t) e^{-\sqrt{\beta}t}$. We observe that

$$\begin{aligned} & \int \langle \nabla \Phi_t, \partial_t \nabla \Phi_t \rangle \rho_t dx - \frac{1}{2} \int \|\nabla \Phi_t\|^2 \nabla \cdot (\rho_t \nabla \Phi_t) dx \\ & \quad - \int \frac{\delta E}{\delta \rho_t} \nabla \cdot (\rho_t \nabla \Phi_t) \rho_t dx \\ &= \int \left\langle \partial_t \nabla \Phi_t + \frac{1}{2} \nabla \|\nabla \Phi_t\|^2 + \nabla \frac{\delta E}{\delta \rho_t}, \nabla \Phi_t \right\rangle \rho_t dx \\ &= -2\sqrt{\beta} \int \|\nabla \Phi_t\|^2 \rho_t dx, \end{aligned} \quad (33)$$

where the last equality uses (W-AIG) with $\alpha_t = 2\sqrt{\beta}$. Substituting (32) and (33) into the expression of $\dot{\mathcal{E}}(t)e^{-\sqrt{\beta}t}$ yields

$$\begin{aligned}\dot{\mathcal{E}}(t)e^{-\sqrt{\beta}t} &\leq \beta \int \langle \partial_t T_t, T_t(x) - x \rangle \rho_t dx - \frac{\beta}{2} \int \|T_t(x) - x\|^2 \nabla \cdot (\rho_t \nabla \Phi_t) dx \\ &\quad - \beta \int \langle T_t(x) - x, \nabla \Phi_t \rangle \rho_t dx - \sqrt{\beta} \int \langle \partial_t T_t, \nabla \Phi_t \rangle \rho_t dx \\ &\quad - \sqrt{\beta} \int \langle T_t(x) - x, \partial_t \nabla \Phi_t \rangle \rho_t dx - \sqrt{\beta} \int \left\langle T_t(x) - x, \nabla \frac{\delta E}{\delta \rho_t} \right\rangle \rho_t dx \\ &\quad + \sqrt{\beta} \int \langle T_t(x) - x, \nabla \Phi_t \rangle \nabla \cdot (\rho_t \nabla \Phi_t) dx - \frac{3\sqrt{\beta}}{2} \int \|\nabla \Phi_t\|^2 \rho_t dx.\end{aligned}\tag{34}$$

Then, we deal with the terms with $\nabla \cdot (\rho_t \nabla \Phi_t)$. We have the following two identities

$$\begin{aligned}&\int \langle T_t(x) - x, \nabla \Phi_t \rangle \nabla \cdot (\rho_t \nabla \Phi_t) dx \\ &= - \int \langle \nabla \langle T_t(x) - x, \nabla \Phi_t \rangle, \nabla \Phi_t \rangle \rho_t dx \\ &= - \int \langle \nabla \Phi_t, \nabla^2 \Phi_t(x) (T_t(x) - x) + (\nabla T_t - I) \nabla \Phi_t \rangle \rho_t dx \\ &= - \frac{1}{2} \int \langle T_t(x) - x, \nabla \|\nabla \Phi_t\|^2 \rangle \rho_t dx - \int \langle \nabla \Phi_t, \nabla T_t \nabla \Phi_t \rangle \rho_t dx + \int \|\nabla \Phi_t\|^2 \rho_t dx.\end{aligned}\tag{35}$$

$$\begin{aligned}&\quad - \frac{1}{2} \int \|T_t(x) - x\|^2 \nabla \cdot (\rho_t \nabla \Phi_t) dx \\ &= \int \langle (\nabla T_t(x) - I)(T_t(x) - x), \nabla \Phi_t \rangle \rho_t dx \\ &= \int \langle T_t(x) - x, \nabla T_t \nabla \Phi_t \rangle \rho_t dx - \int \langle T_t(x) - x, \nabla \Phi_t \rangle \rho_t dx.\end{aligned}\tag{36}$$

Hence, we can proceed to compute the terms with the coefficient $\sqrt{\beta}$. (29) and (35) yields

$$\begin{aligned}&- \sqrt{\beta} \int \langle \partial_t T_t, \nabla \Phi_t \rangle \rho_t dx - \sqrt{\beta} \int \left\langle T_t(x) - x, \partial_t \nabla \Phi_t + \nabla \frac{\delta E}{\delta \rho_t} \right\rangle \rho_t dx \\ &\quad - \frac{3\sqrt{\beta}}{2} \int \|\nabla \Phi_t\|^2 \rho_t dx + \sqrt{\beta} \int \langle T_t(x) - x, \nabla \Phi_t \rangle \nabla \cdot (\rho_t \nabla \Phi_t) dx \\ &= - \sqrt{\beta} \int \langle \partial_t T_t + \nabla T_t \nabla \Phi_t, \nabla \Phi_t \rangle \rho_t dx - \frac{\sqrt{\beta}}{2} \int \|\nabla \Phi_t\|^2 \rho_t dx \\ &\quad - \sqrt{\beta} \int \left\langle T_t(x) - x, \partial_t \nabla \Phi_t + \nabla \frac{\delta E}{\delta \rho} + \frac{1}{2} \nabla \|\nabla \Phi_t\|^2 \right\rangle \rho_t dx \\ &\leq - \frac{\sqrt{\beta}}{2} \int \|\nabla \Phi_t\|^2 \rho_t dx + 2\beta \int \langle T_t(x) - x, \nabla \Phi_t \rangle \rho_t dx.\end{aligned}\tag{37}$$

Substituting (36) and (37) into (34) gives

$$\begin{aligned}&\dot{\mathcal{E}}(t)e^{-\sqrt{\beta}t} + \frac{\sqrt{\beta}}{2} \int \|\nabla \Phi_t\|^2 \rho_t dx \\ &\leq \beta \int \langle \partial_t T_t, T_t(x) - x \rangle \rho_t dx - \frac{\beta}{2} \int \|T_t(x) - x\|^2 \nabla \cdot (\rho_t \nabla \Phi_t) dx \\ &\quad - \beta \int \langle T_t(x) - x, \nabla \Phi_t \rangle \rho_t dx + 2\beta \int \langle T_t(x) - x, \nabla \Phi_t \rangle \rho_t dx \\ &= \beta \int \langle \partial_t T_t + \nabla T_t \nabla \Phi_t, T_t(x) - x \rangle \rho_t dx = 0,\end{aligned}$$

where the last equality uses (30). In summary, we have

$$\dot{\mathcal{E}}(t)e^{-\sqrt{\beta}t} \leq - \frac{\sqrt{\beta}}{2} \int \|\nabla \Phi_t\|^2 \rho_t dx \leq 0.$$

Proof of Proposition 5. Differentiating $\mathcal{E}(t)$ w.r.t. t , we compute that

$$\begin{aligned}
\dot{\mathcal{E}}(t) &= \int \langle \partial_t T_t, T_t(x) - x \rangle \rho_t dx - \frac{1}{2} \int \|T_t(x) - x\|^2 \nabla \cdot (\rho_t \nabla \Phi_t) dx \\
&\quad - \int \left\langle \partial_t T_t, \frac{t}{2} \nabla \Phi_t \right\rangle \rho_t dx - \int \left\langle T_t(x) - x, \frac{1}{2} \nabla \Phi_t + \frac{t}{2} \partial_t \nabla \Phi_t \right\rangle \rho_t dx \\
&\quad + \int \left\langle T_t(x) - x, \frac{t}{2} \nabla \Phi_t \right\rangle \nabla \cdot (\rho_t \nabla \Phi_t) dx + \int \left\langle \frac{t}{2} \nabla \Phi_t, \frac{1}{2} \nabla \Phi_t + \frac{t}{2} \partial_t \nabla \Phi_t \right\rangle \rho_t dx \\
&\quad - \frac{1}{2} \int \left\| \frac{t}{2} \nabla \Phi_t \right\|^2 \nabla \cdot (\rho_t \nabla \Phi_t) dx - \frac{t^2}{4} \int \frac{\delta E}{\delta \rho_t} \nabla \cdot (\rho_t \nabla \Phi_t) dx + \frac{t}{2} (E(\rho_t) - E(\rho^*)).
\end{aligned} \tag{38}$$

Because $E(\rho)$ is Hess(0), Proposition 6 yields

$$E(\rho_t) = E(\rho_t) - E(\rho^*) \leq - \int \left\langle T_t(x) - x, \nabla \frac{\delta E}{\delta \rho_t} \right\rangle \rho_t dx. \tag{39}$$

Utilizing the inequality (39) and substituting the expressions of terms involving $\partial_t T_t$ and $\nabla \cdot (\rho_t \nabla \Phi_t)$ in (38) with the expressions in (29) (30) and (35) (36), we obtain

$$\begin{aligned}
\dot{\mathcal{E}}(t) &\leq - \int \langle \nabla \Phi_t, \nabla T_t(x) (T_t(x) - x) \rangle \rho_t dx + \int \langle T_t(x) - x, \nabla T_t \nabla \Phi_t \rangle \rho_t dx \\
&\quad - \int \langle T_t(x) - x, \nabla \Phi_t \rangle \rho_t dx + \frac{t}{2} \int \langle \nabla \Phi_t, \nabla T_t \nabla \Phi_t \rangle \rho_t dx \\
&\quad - \frac{1}{2} \int \langle T_t(x) - x, \nabla \Phi_t \rangle \rho_t dx - \frac{t}{2} \int \langle \partial_t \nabla \Phi_t, T_t(x) - x \rangle \rho_t dx \\
&\quad - \frac{t}{4} \int \langle T_t(x) - x, \nabla \|\nabla \Phi_t\|^2 \rangle \rho_t dx - \frac{t}{2} \int \langle \nabla \Phi_t, \nabla T_t \nabla \Phi_t \rangle \rho_t dx \\
&\quad + \frac{t}{2} \int \|\nabla \Phi_t\|^2 \rho_t dx + \frac{t}{4} \int \|\nabla \Phi_t\|^2 \rho_t dx + \frac{t^2}{4} \int \langle \nabla \Phi_t, \partial_t \nabla \Phi_t \rangle \rho_t dx \\
&\quad + \frac{t^2}{8} \int \langle \nabla \Phi_t, \nabla \|\nabla \Phi_t\|^2 \rangle \rho_t dx + \frac{t^2}{4} \int \left\langle \nabla \Phi_t, \nabla \frac{\delta E}{\delta \rho_t} \right\rangle \rho_t dx \\
&\quad - \frac{t}{2} \int \left\langle T_t(x) - x, \nabla \frac{\delta E}{\delta \rho_t} \right\rangle \rho_t dx.
\end{aligned} \tag{40}$$

The expression of (40) can be reformulated into

$$\begin{aligned}
\dot{\mathcal{E}}(t) &\leq - \frac{3}{2} \int \langle T_t(x) - x, \nabla \Phi_t \rangle \rho_t dx + \frac{3t}{4} \int \|\nabla \Phi_t\|^2 \rho_t dx \\
&\quad - \frac{t}{2} \int \left\langle T_t(x) - x, \partial_t \nabla \Phi_t + \frac{1}{2} \nabla \|\nabla \Phi_t\|^2 + \nabla \frac{\delta E}{\delta \rho_t} \right\rangle \rho_t dx \\
&\quad + \frac{t^2}{4} \int \left\langle \nabla \Phi_t, \partial_t \nabla \Phi_t + \frac{1}{2} \nabla \|\nabla \Phi_t\|^2 + \nabla \frac{\delta E}{\delta \rho_t} \right\rangle \rho_t dx.
\end{aligned}$$

From (W-AIG) with $\alpha_t = 3/t$, we have the following equalities.

$$\begin{aligned}
\frac{t^2}{4} \int \left\langle \nabla \Phi_t, \partial_t \nabla \Phi_t + \frac{1}{2} \nabla \|\nabla \Phi_t\|^2 + \nabla \frac{\delta E}{\delta \rho_t} \right\rangle \rho_t dx &= - \frac{3t}{4} \int \|\nabla \Phi_t\|^2 \rho_t dx, \\
- \frac{t}{2} \int \left\langle T_t(x) - x, \partial_t \nabla \Phi_t + \frac{1}{2} \nabla \|\nabla \Phi_t\|^2 + \nabla \frac{\delta E}{\delta \rho_t} \right\rangle \rho_t dx &= \frac{3}{2} \int \langle T_t(x) - x, \nabla \Phi_t \rangle \rho_t dx.
\end{aligned}$$

As a result, $\dot{\mathcal{E}}(t) \leq 0$. This completes the proof.

C.5 Comparison with the proof in [32]

The accelerated flow in [32] is given by

$$\frac{dX_t}{dt} = e^{\alpha_t - \gamma_t} Y_t, \quad \frac{dY_t}{dt} = -e^{\alpha_t + \beta_t + \gamma_t} \nabla \left(\frac{\delta E}{\delta \rho_t} \right) (X_t). \tag{41}$$

Here the target distribution satisfies $\rho_\infty(x) = \rho^*(x) \propto \exp(-f(x))$. Suppose that we take $\alpha_t = \log p - \log t$, $\beta_t = p \log t + \log C$ and $\gamma_t = p \log t$. Here we specify $p = 2$ and $C = 1/4$. Then the accelerated flow (41) recovers the particle formulation of W-AIG flows if we replace Y_t by $2t^{-3}V_t$. The Lyapunov function in [32] follows

$$\begin{aligned} V(t) &= \frac{1}{2} \mathbb{E} \left[\|X_t + e^{-\gamma_t} Y_t - T_{\rho_t}^{\rho^*}(X_t)\|^2 \right] + e^{\beta_t} (E(\rho) - E(\rho^*)) \\ &= \frac{1}{2} \mathbb{E} \left[\|X_t + \frac{t}{2} V_t - T_{\rho_t}^{\rho^*}(X_t)\|^2 \right] + \frac{t^2}{4} (E(\rho_t) - E(\rho^*)) \\ &= \frac{1}{2} \int \left\| -(T_t(x) - x) + \frac{t}{2} \nabla \Phi_t(x) \right\|^2 \rho_t(x) dx + \frac{t^2}{4} (E(\rho_t) - E(\rho^*)). \end{aligned}$$

The last equality is based on the fact that $V_t = \nabla \Phi_t(X_t)$ and $T_t = T_{\rho_t}^{\rho^*}$ is the optimal transport plan from ρ_t to ρ^* . This indicates that the Lyapunov function in [32] is identical to ours. The technical assumption in [32] follows

$$\begin{aligned} 0 &= \mathbb{E} \left[\left(X_t + e^{-\gamma_t} Y_t - T_{\rho_t}^{\rho^*}(X_t) \right) \cdot \frac{d}{dt} T_{\rho_t}^{\rho^*}(X_t) \right] \\ &= \mathbb{E} \left[\left(X_t + \frac{t}{2} V_t - T_t(X_t) \right) \cdot \frac{d}{dt} T_t(X_t) \right] \\ &= \mathbb{E} \left[\left(X_t + \frac{t}{2} V_t - T_t(X_t) \right) \cdot ((\partial_t T_t)(X_t) + \nabla T_t V_t) \right] \\ &= \int \left\langle x - T_t(x) + \frac{t}{2} \nabla \Phi_t(x), \partial_t T_t + \nabla T_t \nabla \Phi_t \right\rangle \rho_t dx. \end{aligned}$$

Based on $\partial_t T_t = -\nabla T_t u_t$ and Lemma 3, we have

$$\begin{aligned} & \int \langle x - T_t(x), \partial_t T_t + \nabla T_t \nabla \Phi_t \rangle \rho_t dx \\ &= \int \langle x - T_t(x), \nabla T_t (\nabla \Phi_t - u_t) \rangle \rho_t dx = 0. \\ & \int \langle \nabla \Phi_t, \partial_t T_t + \nabla T_t \nabla \Phi_t \rangle \rho_t dx \\ &= \int \langle \nabla \Phi_t, \nabla T_t (\nabla \Phi_t - u_t) \rangle \rho_t dx \\ &= \int \langle \nabla \Phi_t - u_t, \nabla T_t (\nabla \Phi_t - u_t) \rangle \rho_t dx \geq 0. \end{aligned}$$

As a result, we have

$$\begin{aligned} & \mathbb{E} \left[\left(X_t + e^{-\gamma_t} Y_t - T_{\rho_t}^{\rho_\infty}(X_t) \right) \cdot \frac{d}{dt} T_{\rho_t}^{\rho_\infty}(X_t) \right] \\ &= \frac{t}{2} \int \langle \nabla \Phi_t - u_t, \nabla T_t (\nabla \Phi_t - u_t) \rangle \rho_t dx \geq 0. \end{aligned}$$

In 1-dimensional case, because $\nabla \cdot (\rho_t(u_t - \nabla \Phi_t)) = 0$ indicates that $\rho_t(u_t - \nabla \Phi_t) = 0$. For $\rho_t(x) > 0$, we have $u_t(x) - \nabla \Phi_t(x) = 0$. So the technical assumption holds. In general cases, although $u_t = \partial_t(T_t)^{-1} \circ T_t$ satisfies $\nabla \cdot (\rho_t(u_t - \nabla \Phi_t)) = 0$, but this does not necessary indicate that $u_t = \nabla \Phi_t$. Hence, $\mathbb{E} \left[\left(X_t + e^{-\gamma_t} Y_t - T_{\rho_t}^{\rho_\infty}(X_t) \right) \cdot \frac{d}{dt} T_{\rho_t}^{\rho_\infty}(X_t) \right] = 0$ does not necessary hold except for 1-dimensional case.

D Proof of convergence rate under Fisher-Rao metric

In this section, we present proofs of propositions in Section 4 under Fisher-Rao metric.

D.1 Geodesic curve under the Fisher-Rao metric

We first investigate on the explicit solution of geodesic curve under the Fisher-Rao metric in probability space. The geodesic curve shall satisfy

$$\begin{cases} \partial_t \rho_t - (\Phi_t - \mathbb{E}_{\rho_t}[\Phi_t])\rho_t = 0, \\ \partial_t \Phi_t + \frac{1}{2}\Phi_t^2 - \mathbb{E}_{\rho_t}[\Phi_t]\Phi_t = 0. \end{cases} \quad (42)$$

with initial values $\rho_t|_{t=0} = \rho_0$ and $\Phi_t|_{t=0} = \Phi_0$. The Hamiltonian follows

$$\mathcal{H}(\rho, \Phi) = \frac{1}{2}(\mathbb{E}_{\rho_t}[\Phi_t^2] - (\mathbb{E}_{\rho_t}[\Phi_t])^2).$$

We reparametrize ρ_t by $\rho_t = R_t^2$ with $R_t > 0$ and $\int R_t^2 dx = 1$. Then,

$$\begin{cases} \partial_t R_t - \frac{1}{2}(\Phi_t - \mathbb{E}_{R_t^2}[\Phi_t])R_t = 0, \\ \partial_t \Phi_t + \frac{1}{2}\Phi_t^2 - \mathbb{E}_{R_t^2}[\Phi_t]\Phi_t = 0. \end{cases}$$

Proposition 7 *The solution to (42) with initial values $\rho_t|_{t=0} = \rho_0$ and $\Phi_t|_{t=0} = \Phi_0$ follows*

$$R(x, t) = A(x) \sin(Ht) + B(x) \cos(Ht), \quad (43)$$

where

$$A(x) = \frac{1}{2H} R_0(x) (\Phi_0(x) - \mathbb{E}_{R_0^2}[\Phi_0]), \quad B(x) = R_0(x), \quad (44)$$

and

$$H = \frac{1}{2} \sqrt{\mathbb{E}_{R_0^2}[\Phi_0^2] - (\mathbb{E}_{R_0^2}[\Phi_0])^2}.$$

We also have $\int R_t^2 dx = 1$ for $t \geq 0$.

PROOF We can compute that

$$\begin{aligned} 2\partial_{tt}R_t &= \left(\partial_t \Phi_t - 2 \int R_t \Phi_t \partial_t R_t dx - \mathbb{E}_{R_t^2}[\partial_t \Phi_t] \right) R_t + \partial_t R_t (\Phi_t - \mathbb{E}_{R_t^2}[\Phi_t]) \\ &= \left(-\frac{1}{2}\Phi_t^2 + \frac{1}{2}\mathbb{E}_{R_t^2}[\Phi_t^2] + \mathbb{E}_{R_t^2}[\Phi_t]\Phi_t - \mathbb{E}_{R_t^2}[\Phi_t]^2 \right) R_t \\ &\quad - \mathbb{E}_{R_t^2}[\Phi_t(\Phi_t - \mathbb{E}_{R_t^2}[\Phi_t])]R_t + \frac{1}{2}R_t(\Phi_t - \mathbb{E}_{R_t^2}[\Phi_t])^2 \\ &= \left(-\frac{1}{2}\mathbb{E}_{R_t^2}[\Phi_t^2] + \frac{1}{2}(\mathbb{E}_{R_t^2}[\Phi_t])^2 \right) R_t. \end{aligned}$$

In other words,

$$\partial_{tt}R_t = \left(-\frac{1}{4}\mathbb{E}_{R_t^2}[\Phi_t^2] + \frac{1}{4}\mathbb{E}_{R_t^2}[\Phi_t]^2 \right) R_t.$$

We observe that $\frac{1}{2}\mathbb{E}_{R_t^2}[\Phi_t^2] - \frac{1}{2}\mathbb{E}_{R_t^2}[\Phi_t]^2 = \mathcal{H}(\rho_t, \Phi_t)$ is the Hamiltonian, which is invariant along the geodesic curve. Denote

$$H = \sqrt{\frac{1}{2}\mathcal{H}(\rho_t, \Phi_t)} = \frac{1}{2} \sqrt{\mathbb{E}_{R_0^2}[\Phi_0^2] - (\mathbb{E}_{R_0^2}[\Phi_0])^2}.$$

Then, we have

$$\partial_{tt}R_t = -H^2 R_t,$$

which is a wave equation. We also notice that

$$R_t(x)|_{t=0} = R_0(x), \quad \partial_t R_t(x)|_{t=0} = R_0(x)(\Phi_0(x) - \mathbb{E}_{R_0^2}[\Phi_0]).$$

Hence, R_t is uniquely determined by

$$R_t(x) = A(x) \sin(Ht) + B(x) \cos(Ht),$$

where $A(x)$ and $B(x)$ are given in (44). Finally, we verify that $\int R_t^2 dx = 1$. Actually, we can compute that

$$\begin{aligned}\int A^2(x)dx &= \frac{1}{4H^2} \mathbb{E}_{R_0^2}[(\Phi_0(x) - \mathbb{E}_{R_0^2}[\Phi_0])^2] = 1, \\ \int B^2(x)dx &= \int R_0^2(x)dx = 1, \\ \int A(x)B(x)dx &= \frac{1}{2H} \mathbb{E}_{R_0^2}[\Phi_0(x) - \mathbb{E}_{R_0^2}[\Phi_0]] = 0.\end{aligned}$$

Hence,

$$\begin{aligned}& \int R_t(x)^2 dx \\ &= \sin^2(Ht) \int A^2(x)dx + \cos^2(Ht) \int B^2(x)dx + 2 \sin(Ht) \cos(Ht) \int A(x)B(x)dx \\ &= 1.\end{aligned}$$

Proposition 8 Suppose that $\rho_0, \rho_1 > 0$, $\rho_0 \neq \rho_1$. Then, there exists a geodesic curve $\rho(t)$ with $\rho_t|_{t=0} = \rho_0$ and $\rho_t|_{t=1} = \rho_1$.

PROOF We denote $R_0(x) = \sqrt{\rho_0(x)}$ and $R_1(x) = \sqrt{\rho_1(x)}$. We only need to solve $A(x)$ and $H > 0$ such that

$$R_1(x) = A(x) \sin(H) + R_0(x) \cos(H),$$

We shall have

$$\int R_1(x)R_0(x)dx = \cos(H),$$

which indicates $H = \cos^{-1}(\int R_1(x)R_0(x)dx) \in (0, \pi/2]$. Hence, we have

$$A(x) = \frac{R_1(x) - R_0(x) \cos(H)}{\sin(H)}.$$

We can examine that

$$\int A^2(x)dx = \frac{1 - 2 \cos^2(H) + \cos^2(H)}{\sin^2(H)} = 1.$$

On the other hand, we shall examine that

$$R_t(x) > 0, \quad t \in [0, 1].$$

Indeed,

$$\begin{aligned}R_t(x) &= A(x) \sin(Ht) + R_0(x) \cos(Ht) \\ &= \frac{\sin(Ht)(R_1(x) - R_0(x) \cos(H)) + R_0(x) \cos(Ht) \sin(H)}{\sin(H)} \\ &= \frac{1}{\sin H} (\sin(Ht)R_1(x) + (\cos(Ht) \sin(H) - \sin(Ht) \cos(H))R_0(x)) \\ &= \frac{1}{\sin H} (\sin(Ht)R_1(x) + \sin(H(1-t))R_0(x)) > 0.\end{aligned}$$

Hence, $\rho_t(x) = R_t^2(x)$ is the geodesic curve.

A direct derivation is the Fisher-Rao distance between ρ_0 and ρ_1 . Namely, we can recover Φ_0 by

$$\Phi_0(x) = \frac{2HA(x)}{R_0(x)}.$$

We note that $\mathcal{H}(\rho_t, \Phi_0) = 4H^2$. Hence, we have

$$(\mathcal{D}^{FR}(\rho_0, \rho_1))^2 = \int_0^1 4H^2 dt = 4H^2.$$

Remark 2 The manifold $(\mathcal{P}^+(\Omega), \mathcal{G}^{FR}(\rho))$ is homeomorphic to the manifold $(S^+(\Omega), \mathcal{G}^E(R))$, where $S^+(\Omega) = \{R \in \mathcal{F}(\Omega) : R > 0, \int R^2 dx = 1\}$. Here $(S^+(\Omega), \mathcal{G}^E(R))$ is the submanifold to $\mathbb{L}^2(\Omega)$ equipped with the standard Euclidean metric.

D.2 Convergence analysis

We consider accelerated Fisher-Rao gradient flows

$$\begin{cases} \partial_t \rho_t - (\Phi_t - \mathbb{E}_{\rho_t}[\Phi_t])\rho_t = 0, \\ \partial_t \Phi_t + \alpha_t \Phi_t + \frac{1}{2}\Phi_t^2 - \mathbb{E}_{\rho_t}[\Phi_t]\Phi_t + \frac{\delta E}{\delta \rho_t} = 0. \end{cases} \quad (45)$$

In the sense of R_t , we have

$$\begin{cases} \partial_t R_t - \frac{1}{2}(\Phi_t - \mathbb{E}_{R_t^2}[\Phi_t])R_t = 0, \\ \partial_t \Phi_t + \alpha_t \Phi_t + \frac{1}{2}\Phi_t^2 - \mathbb{E}_{R_t^2}[\Phi_t]\Phi_t + \frac{\delta E}{\delta \rho_t} = 0. \end{cases} \quad (46)$$

Then, we prove the convergence results for β -strongly convex $E(\rho)$. Here we take $\alpha_t = 2\sqrt{\beta}$. Consider the Lyapunov function

$$\begin{aligned} \mathcal{E}(t) = & \frac{e^{\sqrt{\beta}t}}{2} \int |\Phi_t - \mathbb{E}_{R_t^2}[\Phi_t] - \sqrt{\beta}T_t|^2 \rho_t dx \\ & + e^{\sqrt{\beta}t} (E(\rho_t) - E(\rho^*)). \end{aligned}$$

Here we define

$$T_t(x) = \frac{2H_t}{\sin(H_t)} \frac{R^*(x) - R_t(x) \cos(H_t)}{R_t(x)}, \quad H_t = \cos^{-1} \left(\int R_t(x) R^*(x) dx \right).$$

We can rewrite the Lyapunov function as

$$\begin{aligned} \mathcal{E}(t) = & \frac{e^{\sqrt{\beta}t}}{2} \int (\Phi_t - \mathbb{E}_{R_t^2}[\Phi_t])^2 \rho_t dx - \sqrt{\beta} e^{\sqrt{\beta}t} \int (\Phi_t - \mathbb{E}_{R_t^2}[\Phi_t]) T_t \rho_t dx \\ & + \frac{\beta e^{\sqrt{\beta}t}}{2} \int T_t^2 \rho_t dx + e^{\sqrt{\beta}t} (E(\rho_t) - E(\rho^*)). \end{aligned}$$

Remark 3 Here it may be problematic if $R_t(x) = 0$ for some x . But in total,

$$\int T_t^2 \rho_t dx = \int (R_t T_t)^2 dx.$$

is well-defined.

From the definition of convexity in probability space, we derive the following proposition.

Proposition 9 *The β -convexity of $E(\rho)$ indicates that*

$$E(\rho^*) \geq E(\rho_t) + \int \left(\frac{\delta E}{\delta \rho_t} - \mathbb{E}_{\rho_t} \left[\frac{\delta E}{\delta \rho_t} \right] \right) T_t \rho_t dx + \frac{\beta}{2} \int T_t^2 \rho_t dx.$$

For simplicity, we define

$$\mathcal{F}_t[\Psi] = \Psi - \mathbb{E}_{R_t^2}[\Psi].$$

We have

$$\partial_t(\mathcal{F}_t[\Psi]) = \partial_t \Psi - \mathbb{E}_{R_t^2}[\partial_t \Psi] - \int R_t^2 \mathcal{F}_t[\Phi_t] \Psi dx = \mathcal{F}_t[\partial_t \Psi] - \int R_t^2 \mathcal{F}_t[\Phi_t] \Psi dx.$$

Before we perform computations, we establish several identities.

$$\int \mathcal{F}_t[\Psi] R_t^2 dx = 0.$$

$$\int \mathcal{F}_t[\Psi_1] \mathcal{F}_t[\Psi_2] R_t^2 dx = \int \mathcal{F}_t[\Psi_1] \Psi_2 R_t^2 dx = \int \mathcal{F}_t[\Psi_2] \Psi_1 R_t^2 dx.$$

Lemma 4 *We have the following observations:*

$$\int (\partial_t T_t) \mathcal{F}_t[\Phi_t] R_t^2 dx + \frac{1}{2} \int T_t (\mathcal{F}_t[\Phi_t])^2 R_t^2 dx \geq - \int (\mathcal{F}_t[\Phi_t])^2 R_t^2 dx, \quad (47)$$

$$\int (\partial_t T_t) T_t R_t^2 dx = - \int T_t \Phi_t R_t^2 dx - \frac{1}{2} \int T_t^2 \mathcal{F}_t[\Phi_t] R_t^2 dx. \quad (48)$$

PROOF We note that

$$\int T_t^2 R_t^2 dx = 4H_t^2,$$

and

$$\int (\mathcal{F}_t[R^* R_t^{-1}])^2 R_t^2 dx = \frac{\sin^2(H_t)}{4H_t^2} \int T_t^2 R_t^2 dx = \sin(H_t^2).$$

We compute the derivatives as follows:

$$\begin{aligned} \partial_t H_t &= - \frac{1}{\sin H_t} \partial_t \int R_t R^* dx = - \frac{1}{2 \sin H_t} \int R_t R^* \mathcal{F}_t[\Phi_t] dx. \\ \partial_t T_t &= - \frac{1}{\sin H_t} \left(\int R_t R^* \mathcal{F}_t[\Phi_t] dx \right) \frac{\sin(H_t) - H_t \cos(H_t)}{\sin^2(H_t)} (R^* R_t^{-1} - \cos(H_t)) \\ &\quad + \frac{2H_t}{\sin(H_t)} \left(-\frac{1}{2} R^* R_t^{-1} \mathcal{F}_t[\Phi_t] - \frac{1}{2} \int R_t R^* \mathcal{F}_t[\Phi_t] dx \right) \\ &= - \frac{1}{\sin H_t} \left(\int R^* R_t \mathcal{F}_t[\Phi_t] dx \right) \frac{\sin(H_t) - H_t \cos(H_t)}{\sin^2(H_t)} \mathcal{F}_t[R^* R_t^{-1}] \\ &\quad - \frac{H_t}{\sin(H_t)} \left(R^* R_t^{-1} \mathcal{F}_t[\Phi_t] + \int R_t R^* \mathcal{F}_t[\Phi_t] dx \right). \end{aligned}$$

For the first inequality, we have

$$\begin{aligned} &\int (\partial_t T_t) \mathcal{F}_t[\Phi_t] R_t^2 dx \\ &= - \frac{1}{\sin(H_t)} \left(\int R^* R_t \mathcal{F}_t[\Phi_t] dx \right) \frac{\sin(H_t) - H_t \cos(H_t)}{\sin^2(H_t)} \int \mathcal{F}_t[R^* R_t^{-1}] \mathcal{F}_t[\Phi_t] R_t^2 dx \\ &\quad - \frac{H_t}{\sin(H_t)} \int (R^* R_t^{-1} \mathcal{F}_t[\Phi_t]) \mathcal{F}_t[\Phi_t] R_t^2 dx \\ &= - \frac{\sin(H_t) - H_t \cos(H_t)}{\sin^3(H_t)} \left(\int \mathcal{F}_t[R^* R_t^{-1}] \mathcal{F}_t[\Phi_t] R_t^2 dx \right)^2 - \frac{1}{2} \frac{2H_t}{\sin(H_t)} \int R^* R_t^{-1} \mathcal{F}_t[\Phi_t] \mathcal{F}_t[\Phi_t] R_t^2 dx \\ &\geq - \frac{\sin(H_t) - H_t \cos(H_t)}{\sin^3(H_t)} \left(\int (\mathcal{F}_t[\Phi_t])^2 R_t^2 dx \right) \left(\int (\mathcal{F}_t[R^* R_t^{-1}])^2 R_t^2 dx \right) \\ &\quad - \frac{1}{2} \frac{2H_t}{\sin(H_t)} \int (R^* R_t^{-1} - \cos(H_t)) (\mathcal{F}_t[\Phi_t])^2 R_t^2 dx - \frac{1}{2} \frac{2H_t}{\sin(H_t)} \int \cos(H_t) (\mathcal{F}_t[\Phi_t])^2 R_t^2 dx \\ &= - \frac{\sin(H_t) - H_t \cos(H_t)}{\sin(H_t)} \left(\int (\mathcal{F}_t[\Phi_t])^2 R_t^2 dx \right) - \frac{1}{2} \int T_t (\mathcal{F}_t[\Phi_t])^2 R_t^2 dx \\ &\quad - \frac{H_t \cos(H_t)}{\sin(H_t)} \int R_t^2 (\mathcal{F}_t[\Phi_t])^2 dx \\ &= - \frac{1}{2} \int T_t (\mathcal{F}_t[\Phi_t])^2 R_t^2 dx - \int (\mathcal{F}_t[\Phi_t])^2 R_t^2 dx. \end{aligned}$$

The inequality is based on Cauchy inequality. For the second inequality, we have

$$\begin{aligned}
& \int (\partial_t T_t) T_t R_t^2 dx \\
&= -\frac{1}{\sin H_t} \left(\int R^* R_t \mathcal{F}_t[\Phi_t] dx \right) \frac{\sin(H_t) - H_t \cos(H_t)}{\sin^2(H_t)} \int T_t \mathcal{F}_t[R^* R_t^{-1}] R_t^2 dx \\
&\quad - \frac{H_t}{\sin(H_t)} \int T_t R^* R_t^{-1} \mathcal{F}_t[\Phi_t] R_t^2 dx \\
&= -\frac{1}{\sin H_t} \left(\int R^* R_t \mathcal{F}_t[\Phi_t] dx \right) \frac{\sin(H_t) - H_t \cos(H_t)}{2 \sin(H_t) H_t} \int T_t^2 R_t^2 dx \\
&\quad - \frac{1}{2} \frac{2H_t}{\sin(H_t)} \int (R^* R_t - \cos(H_t)) T_t \mathcal{F}_t[\Phi_t] R_t^2 dx - \frac{1}{2} \frac{2H_t \cos(H_t)}{\sin(H_t)} \int T_t \mathcal{F}_t[\Phi_t] R_t^2 dx \\
&= -\frac{1}{2H_t} \left(\int T_t \Phi_t R_t^2 dx \right) \frac{\sin(H_t) - H_t \cos(H_t)}{2 \sin(H_t) H_t} \int T_t^2 R_t^2 dx \\
&\quad - \frac{1}{2} \int T_t^2 \mathcal{F}_t[\Phi_t] R_t^2 dx - \frac{H_t \cos(H_t)}{\sin(H_t)} \int T_t \Phi_t R_t^2 dx \\
&= -\left(\frac{\sin(H_t) - H_t \cos(H_t)}{\sin(H_t)} + \frac{H_t \cos(H_t)}{\sin(H_t)} \right) \int T_t \Phi_t R_t^2 dx - \frac{1}{2} \int T_t^2 \mathcal{F}_t[\Phi_t] R_t^2 dx \\
&= -\int T_t \Phi_t R_t^2 dx - \frac{1}{2} \int T_t^2 \mathcal{F}_t[\Phi_t] R_t^2 dx.
\end{aligned}$$

This completes the proof.

Hence, we can compute that

$$\begin{aligned}
e^{-\sqrt{\beta}t} \partial_t \mathcal{E}(t) &= \frac{\sqrt{\beta}}{2} \int (\mathcal{F}_t[\Phi_t])^2 R_t^2 dx + \int \mathcal{F}_t[\Phi_t] \left(\mathcal{F}_t[\partial_t \Phi_t] - \int R_t^2 \mathcal{F}_t[\Phi_t] \Phi_t dx \right) R_t^2 dx \\
&\quad + \frac{1}{2} \int (\mathcal{F}_t[\Phi_t])^2 \mathcal{F}_t[\Phi_t] R_t^2 dx - \beta \int (\Phi_t - \mathbb{E}_{R_t^2}[\Phi_t]) T_t \rho_t dx \\
&\quad - \sqrt{\beta} \int \left(\mathcal{F}_t[\partial_t \Phi_t] - \int R_t^2 \mathcal{F}_t[\Phi_t] \Phi_t dx \right) T_t R_t^2 dx \\
&\quad - \sqrt{\beta} \int \partial_t T_t \mathcal{F}_t[\Phi_t] R_t^2 dx - \sqrt{\beta} \int (\mathcal{F}_t[\Phi_t])^2 T_t R_t^2 dx \\
&\quad + \frac{\beta \sqrt{\beta}}{2} \int T_t^2 R_t^2 dx + \beta \int \partial_t T_t T_t R_t^2 dx + \frac{\beta}{2} \int T_t^2 \mathcal{F}_t[\Phi_t] R_t^2 dx \\
&\quad + \sqrt{\beta} (E(\rho_t) - E(\rho^*)) + \int \mathcal{F}_t[\Phi_t] \mathcal{F}_t \left[\frac{\delta E}{\delta \rho_t} \right] R_t^2 dx.
\end{aligned}$$

From Proposition 9, we have

$$\sqrt{\beta} (E(\rho_t) - E(\rho^*)) + \frac{\beta \sqrt{\beta}}{2} \int T_t^2 R_t^2 dx \leq -\sqrt{\beta} \int \mathcal{F}_t \left[\frac{\delta E}{\delta \rho_t} \right] T_t \rho_t dx.$$

We first compute terms with coefficient β^0 . We have

$$\begin{aligned}
& \int \mathcal{F}_t[\Phi_t] \left(\mathcal{F}_t[\partial_t \Phi_t] - \int R_t^2 \mathcal{F}_t[\Phi_t] \Phi_t dx \right) R_t^2 dx \\
& + \frac{1}{2} \int (\mathcal{F}_t[\Phi_t])^2 \mathcal{F}_t[\Phi_t] R_t^2 dx + \int \mathcal{F}_t[\Phi_t] \mathcal{F}_t \left[\frac{\delta E}{\delta \rho_t} \right] R_t^2 dx \\
& = \int \mathcal{F}_t[\Phi_t] \partial_t \Phi_t R_t^2 dx + \frac{1}{2} \int (\mathcal{F}_t[\Phi_t])^2 \mathcal{F}_t[\Phi_t] R_t^2 dx + \int \mathcal{F}_t[\Phi_t] \frac{\delta E}{\delta \rho_t} R_t^2 dx \\
& = \int \mathcal{F}_t[\Phi_t] \left(-\sqrt{\beta} \Phi_t - \frac{1}{2} \Phi_t^2 + \mathbb{E}_{R_t^2}[\Phi_t] \Phi_t + \frac{1}{2} \mathcal{F}_t[\Phi_t]^2 \right) R_t^2 dx \\
& = \int \mathcal{F}_t[\Phi_t] \left(-\sqrt{\beta} \Phi_t + \frac{1}{2} (\mathbb{E}_{R_t^2}[\Phi_t])^2 \right) R_t^2 dx \\
& = -2\sqrt{\beta} \int \mathcal{F}_t[\Phi_t] \Phi_t R_t^2 dx.
\end{aligned}$$

We then proceed to compute terms with coefficient $\beta^{1/2}$.

$$\begin{aligned}
& \frac{\sqrt{\beta}}{2} \int (\mathcal{F}_t[\Phi_t])^2 R_t^2 dx - \sqrt{\beta} \int \left(\mathcal{F}_t[\partial_t \Phi_t] - \int R_t^2 \mathcal{F}_t[\Phi_t] \Phi_t dx \right) T_t R_t^2 dx \\
& - 2\sqrt{\beta} \int \mathcal{F}_t[\Phi_t] \Phi_t R_t^2 dx - \sqrt{\beta} \int \partial_t T_t \mathcal{F}_t[\Phi_t] R_t^2 dx - \sqrt{\beta} \int (\mathcal{F}_t[\Phi_t])^2 T_t R_t^2 dx \\
& - \sqrt{\beta} \int \mathcal{F}_t \left[\frac{\delta E}{\delta \rho_t} \right] T_t \rho_t dx \\
& = -\frac{3\sqrt{\beta}}{2} \int (\mathcal{F}_t[\Phi_t])^2 R_t^2 dx - \sqrt{\beta} \int \partial_t \Phi_t T_t R_t^2 dx - \sqrt{\beta} \int \partial_t T_t \mathcal{F}_t[\Phi_t] R_t^2 dx \\
& - \sqrt{\beta} \int (\mathcal{F}_t[\Phi_t])^2 T_t R_t^2 dx - \sqrt{\beta} \int \frac{\delta E}{\delta \rho_t} T_t R_t^2 dx \\
& = -\sqrt{\beta} \int T_t R_t^2 \left(\partial_t \Phi_t + \frac{\delta E}{\delta \rho_t} + \frac{1}{2} (\mathcal{F}_t[\Phi_t])^2 \right) - \frac{3\sqrt{\beta}}{2} \int (\mathcal{F}_t[\Phi_t])^2 R_t^2 dx \\
& - \sqrt{\beta} \int \partial_t T_t \mathcal{F}_t[\Phi_t] R_t^2 dx - \frac{\sqrt{\beta}}{2} \int (\mathcal{F}_t[\Phi_t])^2 T_t R_t^2 dx \\
& \leq 2\beta \int T_t \Phi_t R_t^2 - \frac{\sqrt{\beta}}{2} \int (\mathcal{F}_t[\Phi_t])^2 R_t^2 dx.
\end{aligned}$$

The last inequality is based on Lemma 4. Finally, we compute terms with coefficient β :

$$2\beta \int T_t \Phi_t R_t^2 dx - \beta \int \Phi_t T_t R_t^2 dx + \beta \int \partial_t T_t T_t R_t^2 dx + \frac{\beta}{2} \int T_t^2 \mathcal{F}_t[\Phi_t] R_t^2 dx = 0.$$

In summary, we have

$$e^{-\sqrt{\beta}t} \partial_t \mathcal{E}(t) \leq -\frac{\sqrt{\beta}}{2} \int (\mathcal{F}_t[\Phi_t])^2 R_t^2 dx \leq 0.$$

For convex $E(\rho)$, we let $\alpha_t = 3/t$. Consider

$$\mathcal{E}(t) = \frac{1}{2} \int \left(-T_t + \frac{t}{2} \Phi_t \right)^2 R_t^2 dx + \frac{t^2}{4} (E(R_t^2) - E(\rho^*)).$$

We can compute that

$$\begin{aligned}
\dot{E}(t) &= \int (\partial_t T_t) T_t R_t^2 dx + \frac{1}{2} \int T_t^2 \mathcal{F}[\Phi_t] R_t^2 dx - \frac{1}{2} \int T_t \Phi_t R_t^2 dx \\
&\quad - \frac{t}{2} \int T_t (\partial_t \Phi_t) R_t^2 dx - \frac{t}{2} \int (\partial_t T_t) \Phi_t R_t^2 dx \\
&\quad - \frac{t}{2} \int T_t (\mathcal{F}_t[\Phi_t])^2 R_t^2 dx + \frac{t}{4} \int (\mathcal{F}_t[\Phi_t])^2 R_t^2 dx \\
&\quad + \frac{t^2}{4} \int (\partial_t \mathcal{F}_t[\Phi_t]) \mathcal{F}_t[\Phi_t] R_t^2 dx + \frac{t^2}{8} \int (\mathcal{F}_t[\Phi_t])^3 R_t^2 dx \\
&\quad - \frac{t^2}{4} \int \mathcal{F}_t \left[\frac{\delta E}{\delta \rho_t} \right] \mathcal{F}_t[\Phi_t] R_t^2 dx + \frac{t}{2} (E(R_t^2) - E(\rho^*)).
\end{aligned}$$

Because $E(\rho)$ is convex, we have

$$E(R_t^2) - E(\rho^*) \leq - \int \mathcal{F}_t \left[\frac{\delta E}{\delta \rho_t} \right] T_t R_t^2 dx.$$

From Lemma 4, we have

$$\begin{aligned}
\dot{E}(t) &\leq - \frac{3}{2} \int T_t \Phi_t R_t^2 dx - \frac{t}{2} \int T_t (\partial_t \Phi_t) R_t^2 dx \\
&\quad - \frac{t}{4} \int T_t (\mathcal{F}_t[\Phi_t])^2 R_t^2 dx + \frac{3t}{4} \int (\mathcal{F}_t[\Phi_t])^2 R_t^2 dx \\
&\quad + \frac{t^2}{4} \int (\partial_t \Phi_t) \mathcal{F}_t[\Phi_t] R_t^2 dx + \frac{t^2}{8} \int (\mathcal{F}_t[\Phi_t])^3 R_t^2 dx \\
&\quad - \frac{t^2}{4} \int \frac{\delta E}{\delta \rho_t} \mathcal{F}_t[\Phi_t] R_t^2 dx - \frac{t}{2} \int \mathcal{F}_t \left[\frac{\delta E}{\delta \rho_t} \right] T_t R_t^2 dx \\
&= - \frac{3}{2} \int T_t \Phi_t R_t^2 dx - \frac{t}{2} \int T_t R_t^2 \left(\partial_t \Phi_t + \frac{1}{2} (\mathcal{F}_t[\Phi_t])^2 + \frac{\delta E}{\delta \rho_t} \right) \\
&\quad + \frac{3t}{4} \int (\mathcal{F}_t[\Phi_t])^2 R_t^2 dx + \frac{t^2}{4} \int \mathcal{F}_t[\Phi_t] R_t^2 \left(\partial_t \Phi_t + \frac{1}{2} (\mathcal{F}_t[\Phi_t])^2 + \frac{\delta E}{\delta \rho_t} \right) dx \\
&= 0.
\end{aligned}$$

The last equality utilize the fact that $\partial_t \Phi_t + \frac{1}{2} (\mathcal{F}_t[\Phi_t])^2 + \frac{\delta E}{\delta \rho_t} = -\frac{3}{t} \Phi_t$.

E Discrete-time algorithm of AIG flows

In this section, we introduce the discrete-time algorithm for Kalman-Wasserstein AIG flows and Stein AIG flows. Here $E(\rho)$ is the KL divergence from ρ to $\rho^* \propto \exp(-f)$.

E.1 Discrete-time algorithm of KW-AIG flows

For KL divergence, the particle formulation (23) of KW-AIG flows writes

$$\begin{cases} dX_t = C^\lambda(\rho_t) V_t dt, \\ dV_t = -\alpha_t V_t dt - \mathbb{E}[V_t V_t^T](X_t - \mathbb{E}[X_t]) dt - (f(X_t) + \nabla \log \rho_t(X_t)) dt. \end{cases} \quad (49)$$

Consider a particle system $\{X_0^i\}_{i=1}^N$. In k -th iteration, the update rule follows: for $i = 1, 2, \dots, N$,

$$\begin{cases} X_{k+1}^i = X_k^i + \sqrt{\tau_k} C_k^\lambda V_k, \\ V_{k+1} = \alpha_k V_k - \sqrt{\tau_k} \left[\sum_{i=1}^N (V_k^i)(V_k^i)^T \right] (X_k^i - m_k) - \sqrt{\tau_k} (f(X_k^i) + \xi_k(X_k^i)). \end{cases} \quad (50)$$

Here ξ_k is an approximation of $\nabla \log \rho_k$ and we denote

$$m_k = \frac{1}{N} \sum_{i=1}^N X_k^i, \quad C_k^\lambda = \frac{1}{N-1} \sum_{i=1}^N (X_k^i - m_k)(X_k^i - m_k)^T + \lambda I.$$

The choice of α_k is similar to the discrete-time algorithm of W-AIG flows. If $E(\rho)$ is β -strongly convex, then $\alpha_k = \frac{1-\sqrt{\beta\tau_k}}{1+\sqrt{\beta\tau_k}}$; if $E(\rho)$ is convex or β is unknown, then $\alpha_k = \frac{k-1}{k+2}$.

About the adaptive restart technique, the restarting criterion follows

$$\varphi_k = - \sum_{i=1}^N \langle C_k^\lambda V_{k+1}^i, \nabla f(X_k^i) + \xi_k(X_k^i) \rangle. \quad (51)$$

The overall algorithm is summarized as follows.

Algorithm 2 Discrete-time particle implementation of KW-AIG flow

Require: initial positions $\{X_0^i\}_{i=1}^N$, step size τ_k , number of iteration L .

- 1: Set $k = 0$, $V_0^i = 0$, $i = 1, \dots, N$. Set the bandwidth h_0 by MED.
 - 2: **for** $l = 1, 2, \dots, L$ **do**
 - 3: Compute h_l based on BM method: $h_l = \text{BM}(h_{l-1}, \{X_k^i\}_{i=1}^N, \sqrt{\tau})$.
 - 4: Calculate $\xi_k(X_k^i)$ as an approximation of $\nabla \log \rho_k(X_k^i)$.
 - 5: For $i = 1, 2, \dots, N$, update V_{k+1}^i and X_{k+1}^i by (50).
 - 6: Compute φ_k by (51).
 - 7: If $\varphi_k < 0$, set $X_0^i = X_k^i$ and $V_0^i = 0$ and $k = 0$; otherwise set $k = k + 1$.
 - 8: **end for**
-

E.2 Discrete-time algorithm for S-AIG flows

For KL divergence, the particle formulation of S-AIG flows writes

$$\begin{cases} \frac{d}{dt} X_t = \int k(X_t, y) \nabla \Phi_t(y) \rho_t(y) dy, \\ \frac{d}{dt} V_t = -\alpha_t V_t - \int V_t^T \nabla \Phi_t(y) \nabla_x k(X_t, y) \rho_t(y) dy - \nabla f(X_t) - \nabla \log \rho_t. \end{cases} \quad (52)$$

Consider a particle system $\{X_0^i\}_{i=1}^N$. In k -th iteration, the update rule follows: for $i = 1, 2, \dots, N$,

$$\begin{cases} X_{k+1}^i = X_k^i + \frac{\sqrt{\tau_k}}{N} \sum_{j=1}^N k(X_k^i, X_k^j) V_{k+1}^j, \\ V_{k+1}^i = \alpha_k V_k^i - \frac{\sqrt{\tau_k}}{N} \sum_{j=1}^N (V_k^j)^T V_k^j \nabla_x k(X_k^i, X_k^j) - \sqrt{\tau_k} (\nabla f(X_k^i) + \xi_k(X_k^i)). \end{cases} \quad (53)$$

Here ξ_k is an approximation of $\nabla \log \rho_k$. The choice of α_k is similar, depending on the convexity of $E(\rho)$ w.r.t. Stein metric.

About the adaptive restart technique, the restarting criterion follows

$$\varphi_k = - \sum_{i=1}^N \sum_{j=1}^N k(X_k^j, X_k^i) \langle V_{k+1}^j, \nabla f(X_k^i) + \xi_k(X_k^i) \rangle. \quad (54)$$

The overall algorithm is summarized as follows.

F Implementation details in the numerical experiments

In this section, we provide extra numerical experiments and elaborate on the implementation details in the numerical experiments.

Algorithm 3 Discrete-time particle implementation of S-AIG flow

Require: initial positions $\{X_0^i\}_{i=1}^N$, step size τ_k , number of iteration L .

- 1: Set $k = 0, V_0^i = 0, i = 1, \dots, N$. Set the bandwidth h_0 by MED.
 - 2: **for** $l = 1, 2, \dots, L$ **do**
 - 3: Compute h_l based on BM method: $h_l = \text{BM}(h_{l-1}, \{X_k^i\}_{i=1}^N, \sqrt{\tau})$.
 - 4: Calculate $\xi_k(X_k^i)$ as an approximation of $\nabla \log \rho_k(X_k^i)$.
 - 5: For $i = 1, 2, \dots, N$, update V_{k+1}^i and X_{k+1}^i by (53).
 - 6: Compute φ_k by (54).
 - 7: If $\varphi_k < 0$, set $X_0^i = X_k^i$ and $V_0^i = 0$ and $k = 0$; otherwise set $k = k + 1$.
 - 8: **end for**
-

F.1 Toy examples

We first generate samples from a toy bi-modal distribution in [26]. We compare sampling algorithms based on gradient flows and accelerated gradient flows under Wasserstein metric, Kalman-Wasserstein metric and Stein metric. The number of particles follow $N = 200$. The initial distribution of the particle system follows $\mathcal{N}([0, 10]', I)$.

For the approximation of $\nabla \log \rho_k$, we use a Gaussian kernel and the kernel bandwidth is selected by the BM method. We apply the restart technique for discrete-time algorithms of AIG flows. For W-GF, W-AIG, SVGD and S-AIG, we take the step size $\tau_k = 0.1$. For KW-GF and KW-AIG, we set the regularization parameter $\lambda = 1$ and the step size $\tau_k = 0.02$. We choose a smaller step size for the Kalman-Wasserstein metric because the particle system may blow up for a larger step size. For SVGD and S-AIG, we use a Gaussian kernel with fixed bandwidth 1. The step size of SVGD is adjusted by Adagrad.

From Figure 2, the convergence rate of the particle system depends on the metric. For a fixed metric, samples generated by accelerated gradient flows always converge faster than the ones generated by gradient flows.

F.2 Effect of BM method

We first investigate the validity of the BM method in selecting the bandwidth. The target density ρ^* is a toy bi-modal distribution [26]. We compare two types of particle implementations of the Wasserstein gradient flow over KL divergence:

$$\begin{aligned} X_{k+1}^i &= X_k^i - \tau \nabla f(X_k^i) + \sqrt{2\tau} B_k^i, \\ X_{k+1}^i &= X_k^i - \tau (\nabla f(X_k^i) + \xi_k(X_k^i)). \end{aligned}$$

Here $B_k^i \sim \mathcal{N}(0, 1)$ is the standard Brownian motion and ξ_k is estimated via KDE. The first method is known as the Langevin MCMC method and the second method is called the ParVI method. For ParVI methods, the bandwidth h is selected by MED/HE/BM respectively. The initial distribution of the particle system follows the standard Gaussian $\mathcal{N}(0, I)$. The objective density function follows

$$\begin{aligned} \rho^*(x) &\propto \exp(-2(\|x\| - 3)^2) \\ &\quad \times (\exp(-2(x_1 - 3)^2) + \exp(-2(x_1 + 3)^2)). \end{aligned}$$

All methods run for 200 iterations using the same fixed step size $\tau = 0.1$.

Figure 2 shows the distribution of 200 samples based on different methods. Samples from MCMC match the target distribution in a stochastic way; samples from MED collapse; samples from HE align tidily around contour lines; samples from BM arrange neatly and are closer to samples from MCMC. This indicates that the BM method makes the particle system behave similar to MCMC, though in a deterministic way.

F.3 Details in Subsection 6.1

We follow the same setting as [16], which is also adopted in [14, 13]. The dataset is split into 80% for training and 20% for testing. We use the stochastic gradient and the mini-batch size is taken as

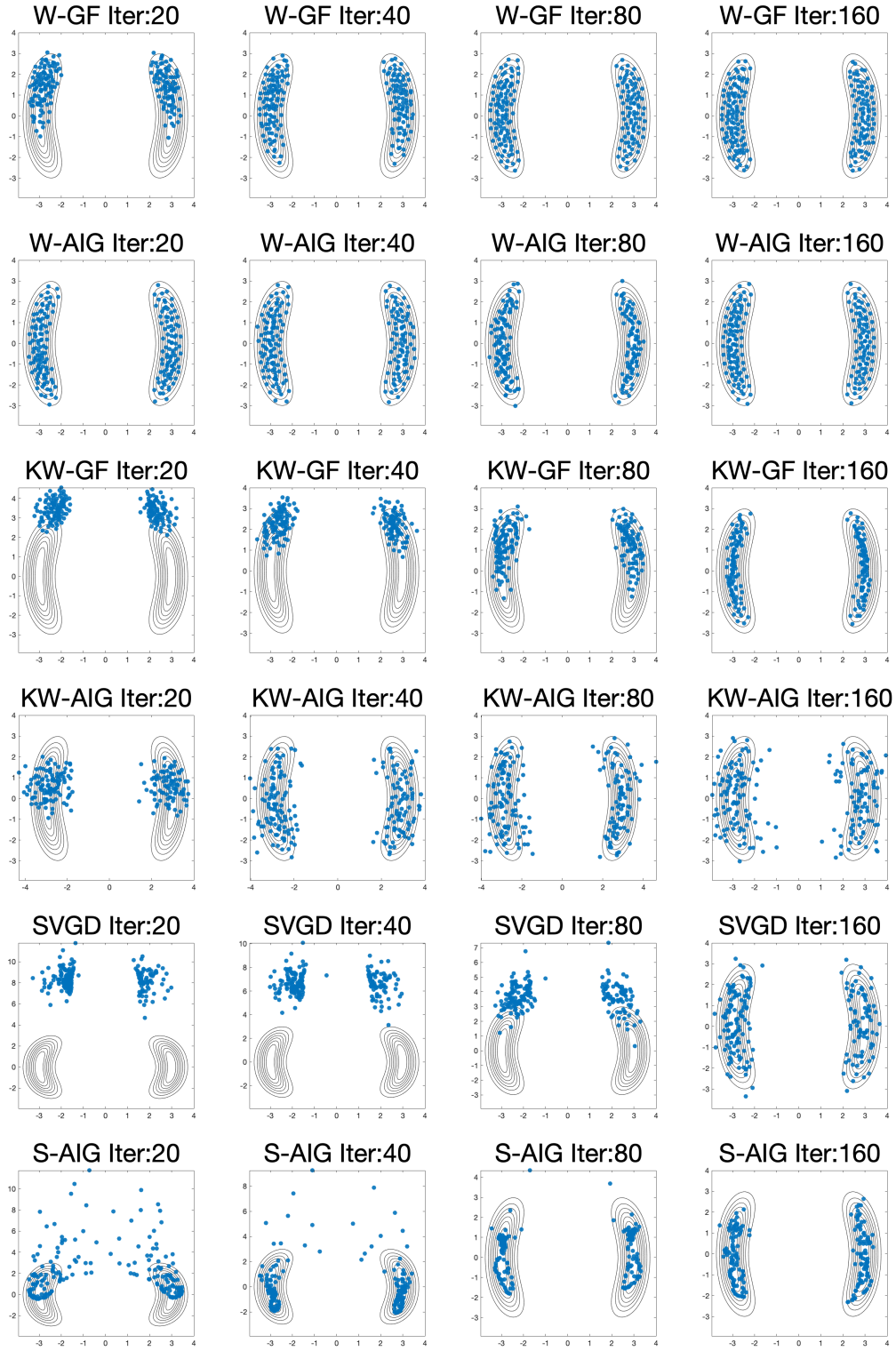


Figure 2: Comparison of different AIG flows on a toy example.

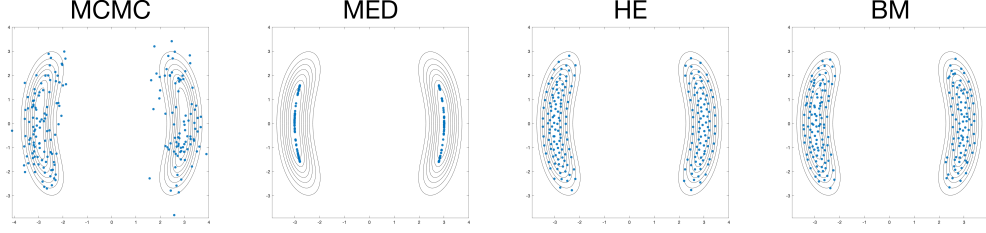


Figure 3: The effect of the BM method. Samples are plotted as blue dots. Left to right: MCMC, MED, HE and BM. All methods are run for 200 iterations with the same initialization.

100. For MCMC, the number of particles is $N = 1000$; for other methods, the number of particles is $N = 100$. The BM method is not applied to SVGD in selecting the bandwidth.

The initial step sizes for the compared methods are given in Table 2, which are selected by grid search over 1×10^i with $i = -3, -4, \dots, -9$. (For SVGD, we use the initial step size in [16].) The step size of SVGD is adjusted by Adagrad, which is same as [16]. For WNAG and WRes, the step size is give by $\tau_l = \tau_0/l^{0.9}$ for $l \geq 1$. The parameters for WNAG and Wnes are identical to [14] and [13]. For other methods, the step size is multiplied by 0.9 every 100 iterations. For methods under Kalman-Wasserstein metric, we require a smaller step size (around $1e-8$) to make the algorithm converge. For all discrete-time algorithms of AIGs, we apply the restart technique. We record the

Method	MCMC	WNAG	Wnes	W-GF	W-AIG	KW-GF	KW-AIG	SVGD	S-AIG
Step size τ_0	$1e-5$	$1e-6$	$1e-5$	$1e-5$	$1e-6$	$1e-7$	$1e-8$	0.05	$1e-5$

Table 2: Initial step sizes for compared algorithms in Bayesian logistic regression.

cpu-time for each method in Table 3. The computational cost of the BM method is much higher than the MED method because we need to evaluate the MMD of two particle systems several times in optimizing the subproblem. We may update the bandwidth using the BM method every 10 iterations to deal with the high computation cost of the BM method. On the other hand, using the MED method for bandwidth, the computational cost of S-AIG is much higher than other methods. This results from the multiple times of computation of particle interacting in updating X_k^i and V_k^i .

Method	MCMC	WNAG	Wnes	W-GF	W-AIG	KW-GF	KW-AIG	SVGD	S-AIG
BM	26.181	164.980	165.407	167.308	170.116	168.711	173.670	7.193	200.016
MED	27.200	7.585	7.688	7.501	7.719	8.847	10.065	7.755	21.303

Table 3: Averaged cpu time(s) cost for algorithms in Bayesian logistic regression.

F.4 Details in Subsection 6.2

We follow the setting of Bayesian neural network as [34]. The kernel bandwidth is adjusted by the MED method. We list the number of epochs and the batch size for each datasets in Table 4. For each dataset, we use 90% of samples as the training set and 10% of samples as the test set. The step size of SVGD is adjusted by Adagrad. For W-GF and W-AIG, the step size is multiplied by 0.64 every 1/10 of total epochs. We select the initial step size by grid search over $\{1, 2, 5\} \times 10^i$ with $i = -3, -4, \dots, -7$ to ensure the best performance of compared methods. We list the initial step sizes for each dataset in Table 5. For W-AIG, we apply the adaptive restart.

Dataset	Boston	Combined	Concrete
Epochs	50	500	500
Batch size	100	100	100
Dataset	Kin8nm	Wine	Year
Epochs	200	20	10
Batch size	100	100	1000

Table 4: Number of epochs and batch size in Bayesian neural network.

Dataset	Boston	Combined	Concrete
AIG	2e-5	2e-4	2e-5
WGF	1e-4	1e-3	2e-5
SVGD	5e-4	5e-3	5e-4
Dataset	Kin8nm	Wine	Year
AIG	2e-5	5e-6	2e-7
WGF	1e-4	1e-4	2e-6
SVGD	5e-3	2e-3	5e-3

Table 5: Initial step sizes for compared methods in Bayesian neural network.

References

- [1] Shun-Ichi Amari. Natural gradient works efficiently in learning. *Neural computation*, 10(2):251–276, 1998.
- [2] Shun-ichi Amari. *Information geometry and its applications*, volume 194. Springer, 2016.
- [3] Shun’ichi Amari, Ole E Barndorff-Nielsen, Robert E Kass, Steffen L Lauritzen, and CR Rao. Differential geometry in statistical inference. IMS, 1987.
- [4] Espen Bernton. Langevin Monte Carlo and JKO splitting. In *Conference On Learning Theory*, pages 1777–1798, 2018.
- [5] José A Carrillo, Young-Pil Choi, and Oliver Tse. Convergence to equilibrium in Wasserstein distance for damped Euler equations with interaction forces. *Communications in Mathematical Physics*, 365(1):329–361, 2019.
- [6] Xiang Cheng, Niladri S Chatterji, Peter L Bartlett, and Michael I Jordan. Underdamped Langevin MCMC: A non-asymptotic analysis. *arXiv preprint arXiv:1707.03663*, 2017.
- [7] Shui-Nee Chow, Wuchen Li, and Haomin Zhou. Wasserstein hamiltonian flows. *arXiv preprint arXiv:1903.01088*, 2019.
- [8] Gustavo Deco and Dragan Obradovic. *An information-theoretic approach to neural computing*. Springer Science & Business Media, 2012.
- [9] A Duncan, N Nüsken, and L Szpruch. On the geometry of stein variational gradient descent. *arXiv preprint arXiv:1912.00894*, 2019.
- [10] Alfredo Garbuno-Inigo, Franca Hoffmann, Wuchen Li, and Andrew M Stuart. Interacting Langevin diffusions: Gradient structure and ensemble Kalman sampler. *arXiv preprint arXiv:1903.08866*, 2019.
- [11] Diederik P Kingma and Jimmy Ba. Adam: A method for stochastic optimization. *arXiv preprint arXiv:1412.6980*, 2014.
- [12] John D Lafferty. The density manifold and configuration space quantization. *Transactions of the American Mathematical Society*, 305(2):699–741, 1988.
- [13] Chang Liu, Jingwei Zhuo, Pengyu Cheng, Ruiyi Zhang, and Jun Zhu. Understanding and accelerating particle-based variational inference. In *International Conference on Machine Learning*, pages 4082–4092, 2019.
- [14] Chang Liu, Jingwei Zhuo, Pengyu Cheng, Ruiyi Zhang, Jun Zhu, and Lawrence Carin. Accelerated first-order methods on the Wasserstein space for Bayesian inference. *arXiv preprint arXiv:1807.01750*, 2018.
- [15] Qiang Liu. Stein variational gradient descent as gradient flow. In I. Guyon, U. V. Luxburg, S. Bengio, H. Wallach, R. Fergus, S. Vishwanathan, and R. Garnett, editors, *Advances in Neural Information Processing Systems 30*, pages 3115–3123. Curran Associates, Inc., 2017.
- [16] Qiang Liu and Dilin Wang. Stein variational gradient descent: A general purpose bayesian inference algorithm. In *Advances in neural information processing systems*, pages 2378–2386, 2016.
- [17] Yuanyuan Liu, Fanhua Shang, James Cheng, Hong Cheng, and Licheng Jiao. Accelerated first-order methods for geodesically convex optimization on Riemannian manifolds. In *Advances in Neural Information Processing Systems*, pages 4868–4877, 2017.

- [18] Yi-An Ma, Niladri Chatterji, Xiang Cheng, Nicolas Flammarion, Peter Bartlett, and Michael I Jordan. Is there an analog of Nesterov acceleration for MCMC? *arXiv preprint arXiv:1902.00996*, 2019.
- [19] Chris J Maddison, Daniel Paulin, Yee Whye Teh, Brendan O’Donoghue, and Arnaud Doucet. Hamiltonian descent methods. *arXiv preprint arXiv:1809.05042*, 2018.
- [20] Luigi Malago, Matteo Matteucci, and Giovanni Pistone. Natural gradient, fitness modelling and model selection: A unifying perspective. In *2013 IEEE Congress on Evolutionary Computation*, pages 486–493. IEEE, 2013.
- [21] James Martens and Roger Grosse. Optimizing neural networks with kronecker-factored approximate curvature. In *International conference on machine learning*, pages 2408–2417, 2015.
- [22] Yurii Nesterov. A method of solving a convex programming problem with convergence rate $O(1/k^2)$. *Soviet Mathematics Doklady*, 27(2):372–376, 1983.
- [23] Felix Otto. The geometry of dissipative evolution equations: the porous medium equation. *Communications in Partial Differential Equations*, 26(1-2):101–174, 2001.
- [24] Brendan O’Donoghue and Emmanuel Candes. Adaptive restart for accelerated gradient schemes. *Foundations of computational mathematics*, 15(3):715–732, 2015.
- [25] Jose C Principe, Dongxin Xu, John Fisher, and Simon Haykin. Information theoretic learning. *Unsupervised adaptive filtering*, 1:265–319, 2000.
- [26] Danilo Jimenez Rezende and Shakir Mohamed. Variational inference with normalizing flows. *arXiv preprint arXiv:1505.05770*, 2015.
- [27] Abhijoy Saha. *A Geometric Framework for Modeling and Inference using the Nonparametric Fisher–Rao metric*. PhD thesis, The Ohio State University, 2019.
- [28] Radhey S Singh. Improvement on some known nonparametric uniformly consistent estimators of derivatives of a density. *The Annals of Statistics*, pages 394–399, 1977.
- [29] Anuj Srivastava and Eric P Klassen. *Functional and shape data analysis*, volume 475. Springer, 2016.
- [30] Andrew M Stuart. Inverse problems: a Bayesian perspective. *Acta numerica*, 19:451–559, 2010.
- [31] Weijie Su, Stephen Boyd., and Emmanuel J. Candès. A differential equation for modeling Nesterov’s accelerated gradient method: Theory and insights. *Journal of Machine Learning Research*, 2016.
- [32] Amirhossein Taghvaei and Prashant G Mehta. Accelerated flow for probability distributions. *arXiv preprint arXiv:1901.03317*, 2019.
- [33] Cédric Villani. *Topics in optimal transportation*. American Mathematical Soc., 2003.
- [34] Dilin Wang, Ziyang Tang, Chandrajit Bajaj, and Qiang Liu. Stein variational gradient descent with matrix-valued kernels. In *Advances in neural information processing systems*, pages 7834–7844, 2019.
- [35] Yifei Wang, Zeyu Jia, and Zaiwen Wen. The Search direction Correction makes first-order methods faster. *arXiv preprint arXiv:1905.06507*, 2019.
- [36] Yifei Wang and Wuchen Li. Information newton’s flow: second-order optimization method in probability space. *arXiv preprint arXiv:2001.04341*, 2020.
- [37] Andre Wibisono. Proximal Langevin Algorithm: Rapid convergence under isoperimetry. *arXiv preprint arXiv:1911.01469*, 2019.
- [38] Hongyi Zhang and Suvrit Sra. Towards Riemannian accelerated gradient methods. *arXiv preprint arXiv:1806.02812*, 2018.